Wide Band and Full Beam Imaging

15th NRAO Synthesis Imaging Workshop

1 – 8 June 2016, Socorro, NM

Urvashi Rau
National Radio Astronomy Observatory

NRAO

Associated Universities, Inc.

New Mexico Tech
SCIENCE · ENGINEERING · RESEARCH · UNIVERSITY

The University of New Mexico

Basic Calibration and Imaging

An interferometer partially measures the spatial Fourier transform of the sky brightness distribution.

$$V_{ij}^{obs}(\nu,t) = M_{ij}(\nu,t) S_{ij}(\nu,t) \iint I(l,m) e^{2\pi i (ul+vm)} dl\, dm$$

Observed visibilities (Data)

Direction Independent Gains

UV sampling pattern

Sky Brightness (Image)

Fourier transform kernel

Standard calibration eliminates $M_{ij}(\nu,t)$

The observed image is a convolution of the PSF with the sky brightness.

$$I^{obs}(l,m) = I^{PSF}(l,m) * I^{sky}(l,m)$$

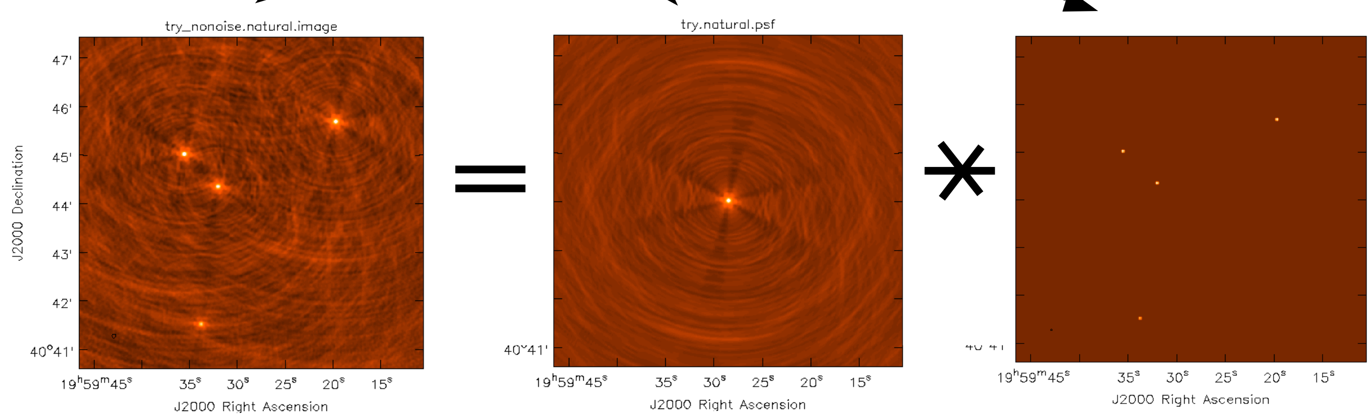

Wide Band and Full Beam Imaging

An interferometer partially measures the spatial Fourier transform of the sky brightness distribution.

$$V_{ij}^{obs}(\nu,t) \approx M_{ij}(\nu,t)\, S_{ij}(\nu,t) \iint I(l,m)\, e^{2\pi i(ul+vm)}\, dl\, dm$$

$$V_{ij}^{obs}(\nu,t) = M_{ij}(\nu,t)\, S_{ij}(\nu,t) \iiint M_{ij}^{s}(l,m,\nu,t)\, I(l,m,\nu,t)\, e^{2\pi i(ul+vm+w(n-1))}\, dl\, dm\, dn$$

Direction Independent Gains

- Eliminated during calibration

Primary Beams

- Power pattern varies with time, frequency and baseline

Sky-brightness varies with frequency (time)

- All sources have spectral structure (some vary with time)

W-Term

-Non-coplanar baselines

-Sky curvature

Direction Dependent Effects

=> The observed image is NOT a simple convolution equation

Wide Band

Wide Field

Full Beam

Wide Band + Full Beam

Example : Imaging the G55 supernova remnant

Summary

Imaging across a wide frequency range

Large bandwidth => Increased 'instantaneous' imaging sensitivity $\sigma_{cont} = \frac{\sigma_{chan}}{\sqrt{N_{chan}}}$

- Angular-resolution increases at higher frequencies
- Sensitivity to large scales decreases at higher frequencies
- Wideband UV-coverage has fewer gaps => lower PSF sidelobe levels

1.0 GHz

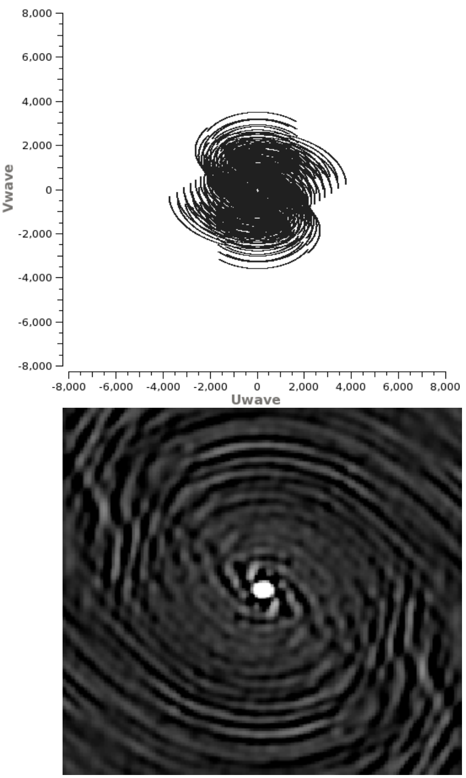

1.5 GHz

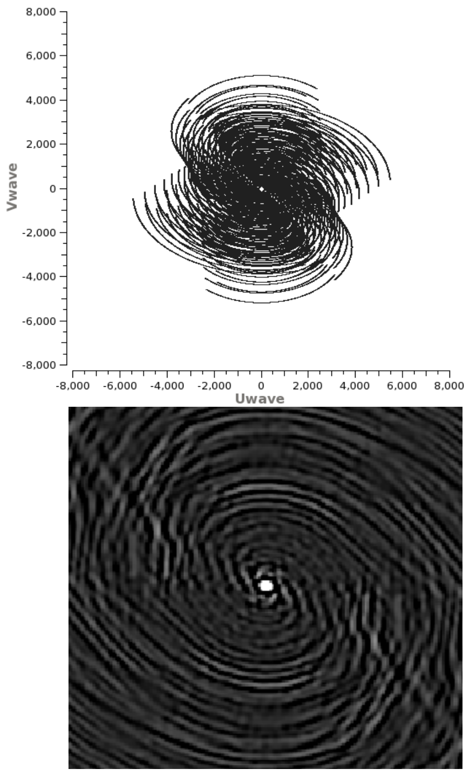

2.0 GHz

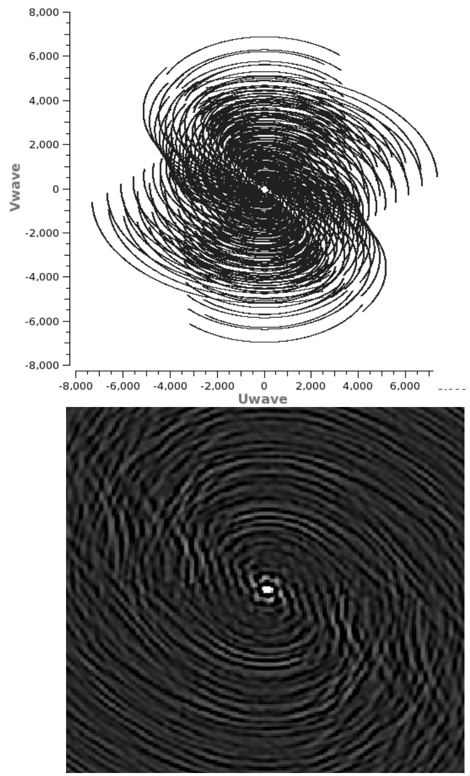

1.0 - 2.0 GHz

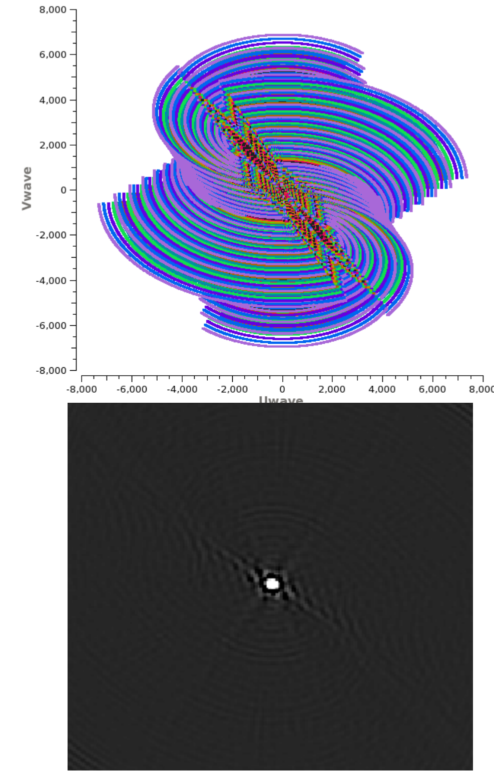

Observed image : $I_\nu^{obs} = I_\nu^{sky} * PSF_\nu$

$$I_{wb}^{obs} = \sum_\nu \left[I_\nu^{sky} * PSF_\nu \right]$$

Algorithms : Cube Imaging & Multi-Frequency Synthesis

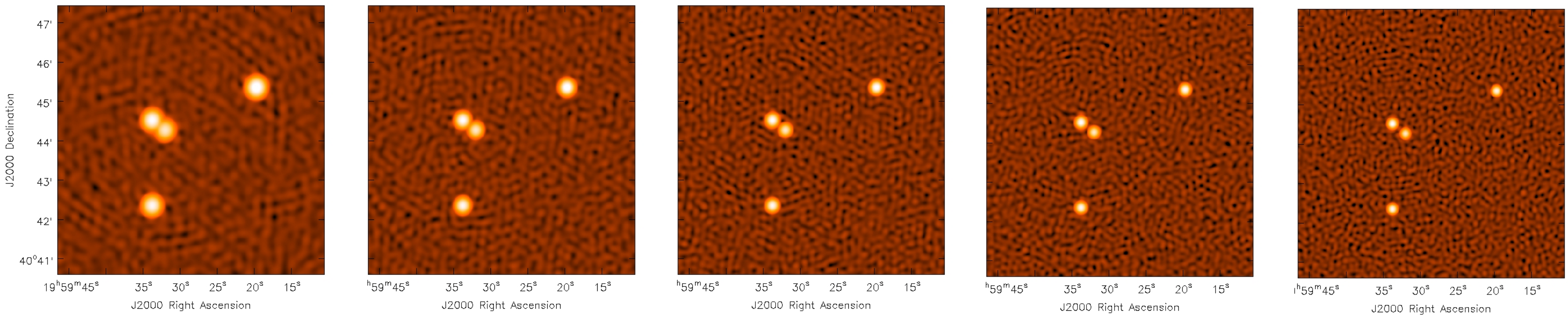

Cube Imaging :

(1) Reconstruct each chan/spw separately
(2) Smooth to the lowest available resolution
(3) Combine to calculate continuum and spectra

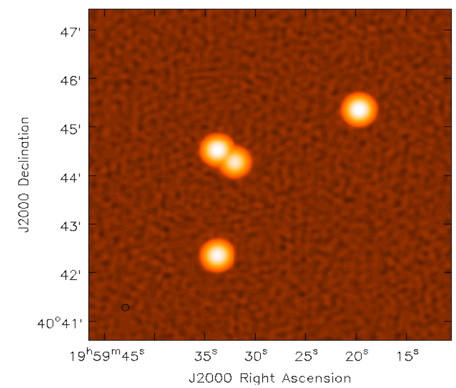

Multi-Frequency-Synthesis :

Combine data from all frequencies onto
a single grid and do a joint reconstruction
(assuming flat sky spectra)

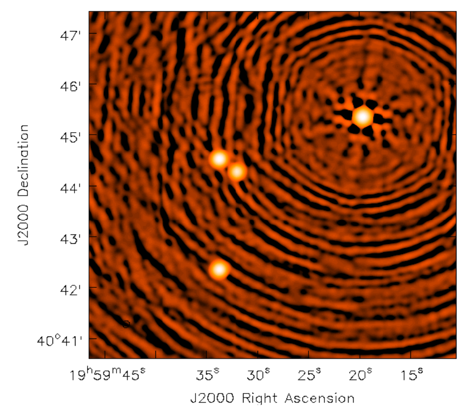

Algorithm : Multi-Term Multi-Frequency-Synthesis

Solve for coefficients of a Taylor polynomial in frequency $I_\nu^{sky} = \sum_t I_t^m \left(\frac{\nu - \nu_0}{\nu_0} \right)^t$

Interpret coefficients as a power-law (spectral index and curvature)

$$I_\nu = I_{\nu_0} \left(\frac{\nu}{\nu_0} \right)^{\alpha + \beta \log(\nu/\nu_0)} \longleftrightarrow \quad I_0^m = I_{\nu_0} \qquad I_1^m = I_{\nu_0} \alpha \qquad I_2^m = I_{\nu_0} \left(\frac{\alpha(\alpha-1)}{2} + \beta \right)$$

Rau &Cornwell, 2011
Sault &Wieringa, 1994

Nterms=1
(ignore spectra)

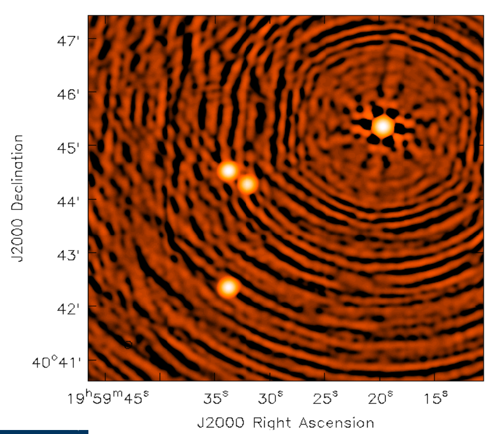

NTerms>1
(Model the spectrum during the reconstruction)

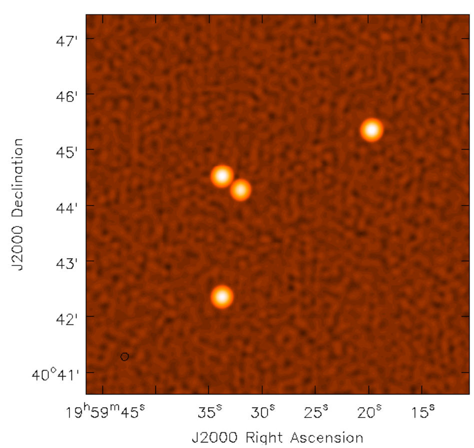

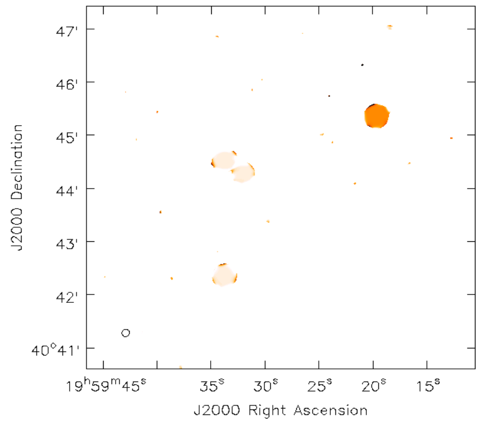

Cube Imaging vs Multi-Frequency-Synthesis

Cube

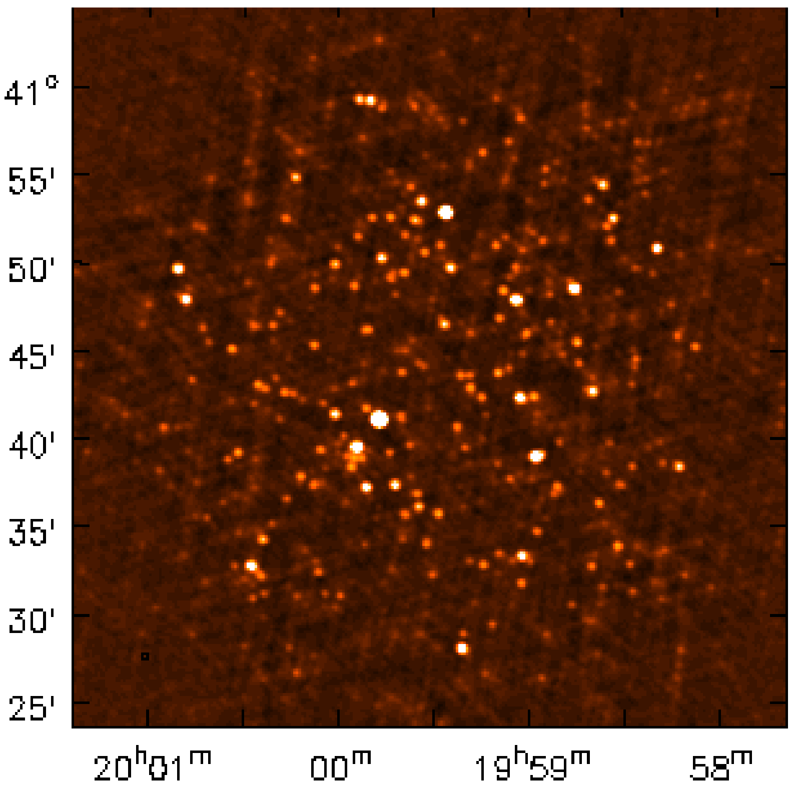

- Low angular resolution
- Weakest sources are not deconvolved enough
- Crowded field may suffer from 'Clean bias' due to PSF sidelobes and require careful masking
+ Independent of spectral model

(MT) MFS

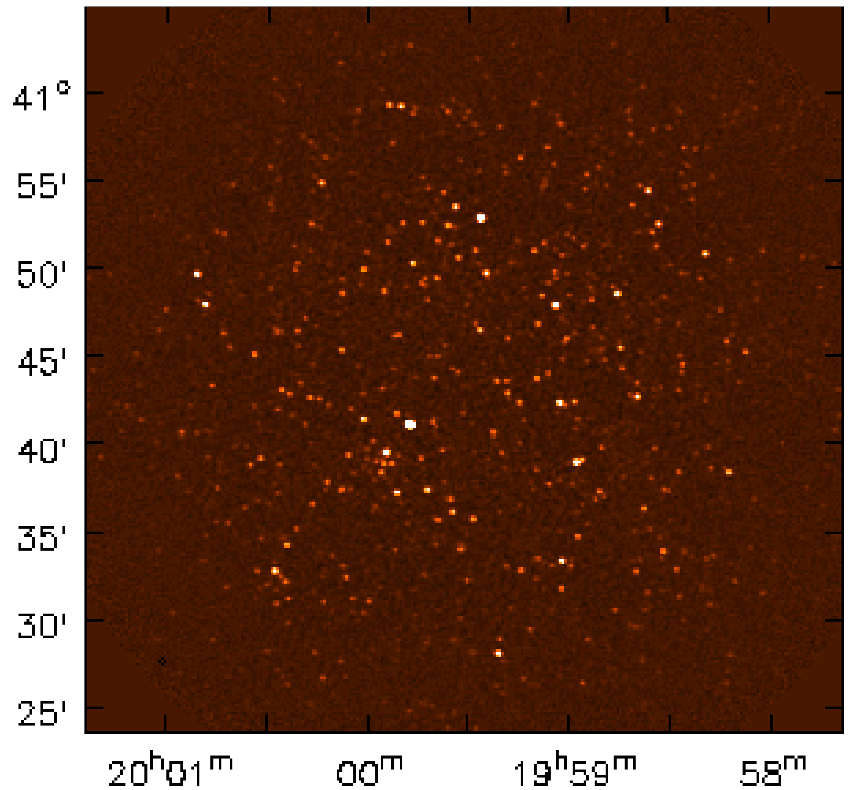

+ High angular resolution
+ Imaging at continuum sensitivity
+ Better PSF and imaging fidelity can eliminate 'Clean bias' and the need for masks in crowded fields
- Depends on how appropriate the spectral model is

Dynamic-range (MT-MFS on 1-2 GHz 3C286 with Nt=1,2,3,4)

NTERMS = 1

Rms :
9 mJy -- 1 mJy

DR :
1600 - 13000

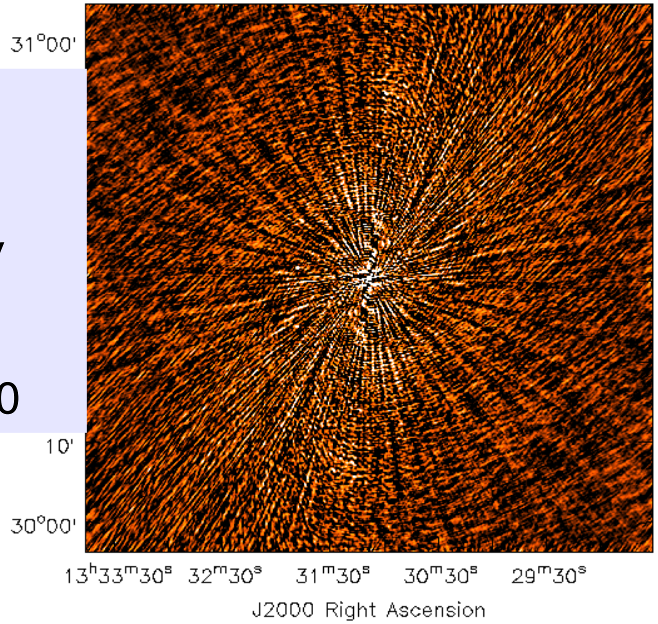

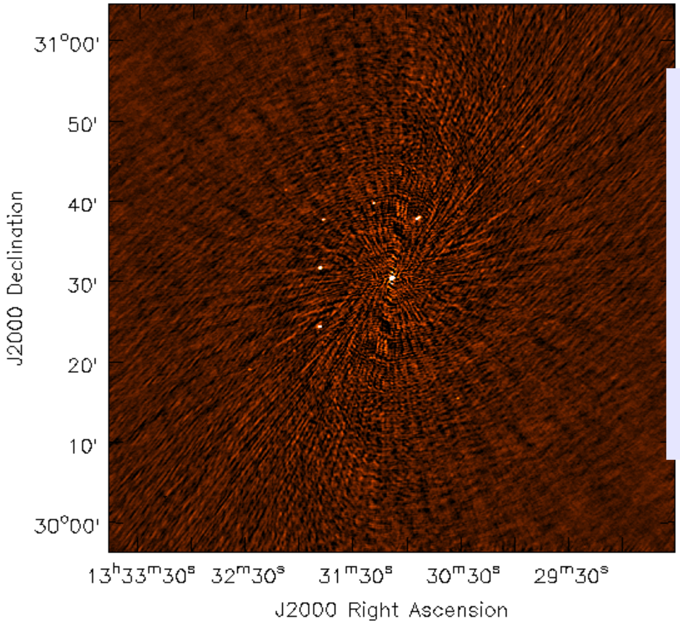

NTERMS = 2

Rms :
1 mJy -- 0.2 mJy

DR :
10,000 - 17,000

NTERMS = 3

Rms :
0.2 mJy -- 85 uJy

DR :
65,000 - 170,000

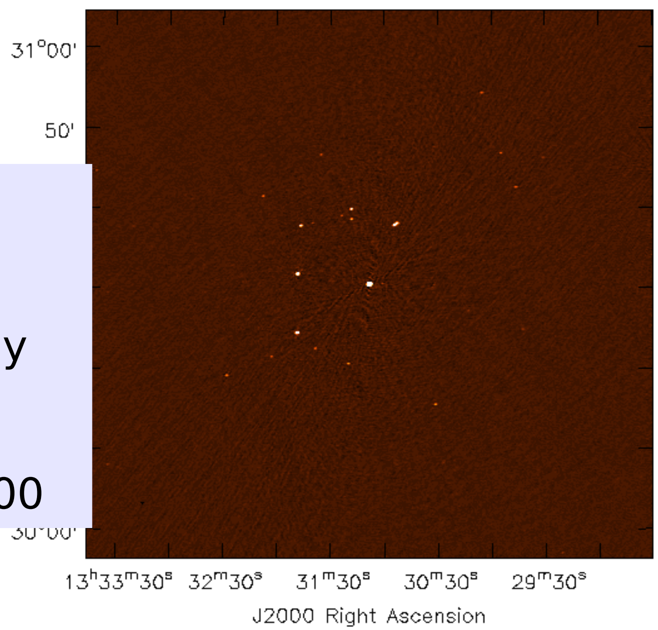

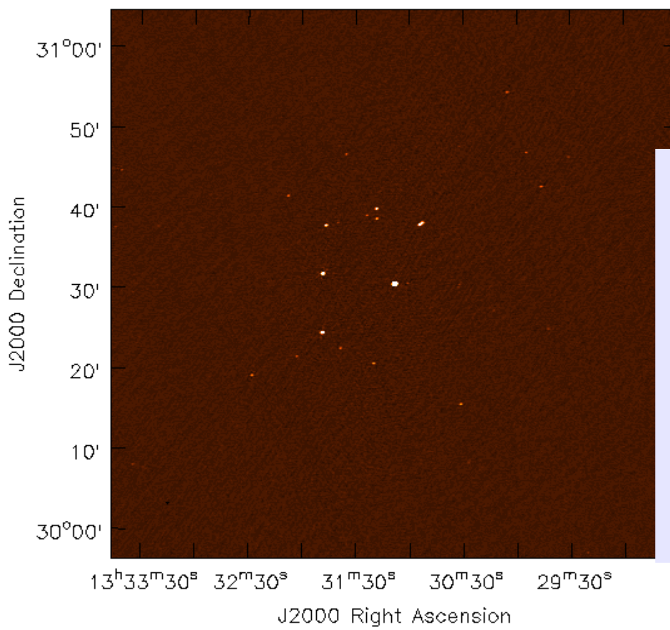

NTERMS = 4

Rms
0.14 mJy -- 80 uJy

DR :
>110,000
- 180,000

Example of MT-MFS imaging on extended-emission

Intensity Image

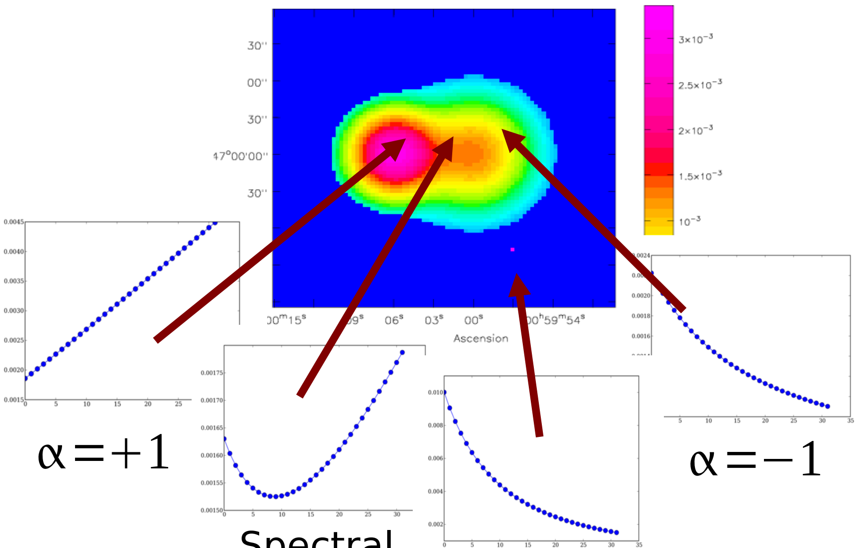

$\alpha = +1$

Spectral Turn-ove
r

$\alpha = -2$

$\alpha = -1$

Average Spectral Index

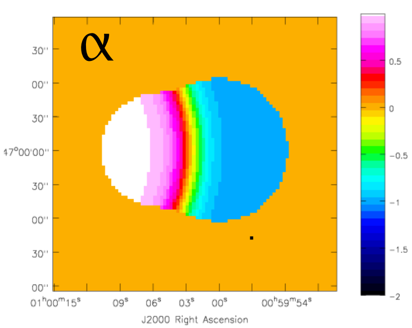

Gradient in Spectral Index

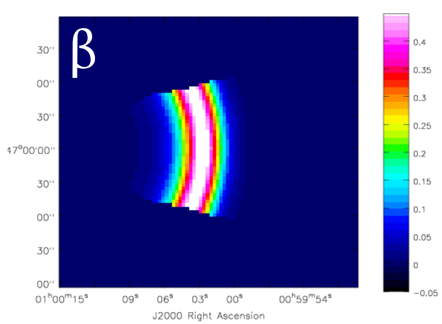

MT-MFS

multi-scale **point-source**

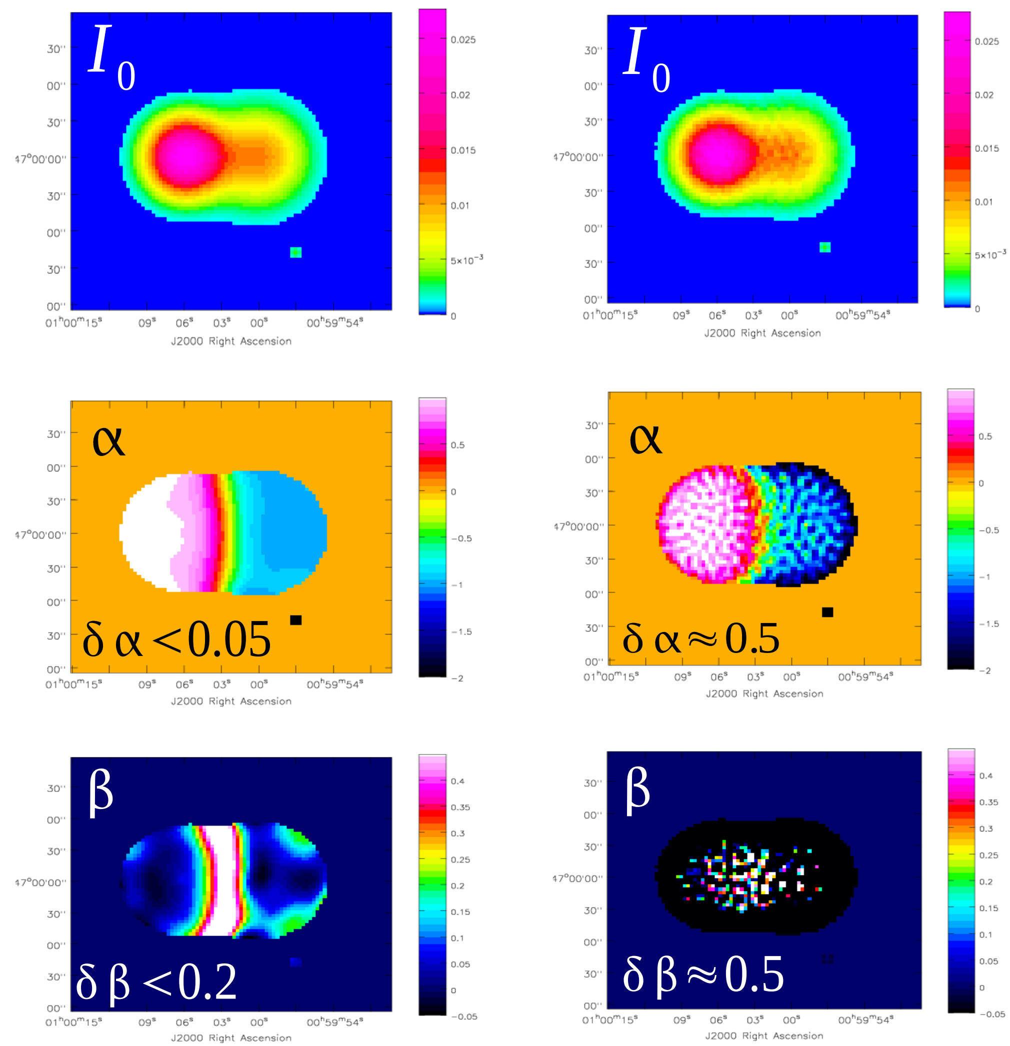

=> Spectral-index error is dominated by 'division between noisy images'
– a multi-scale model gives better spectral index and curvature maps

Supernova Remnants at L and C Band

[Bhatnagar et al, 2011]

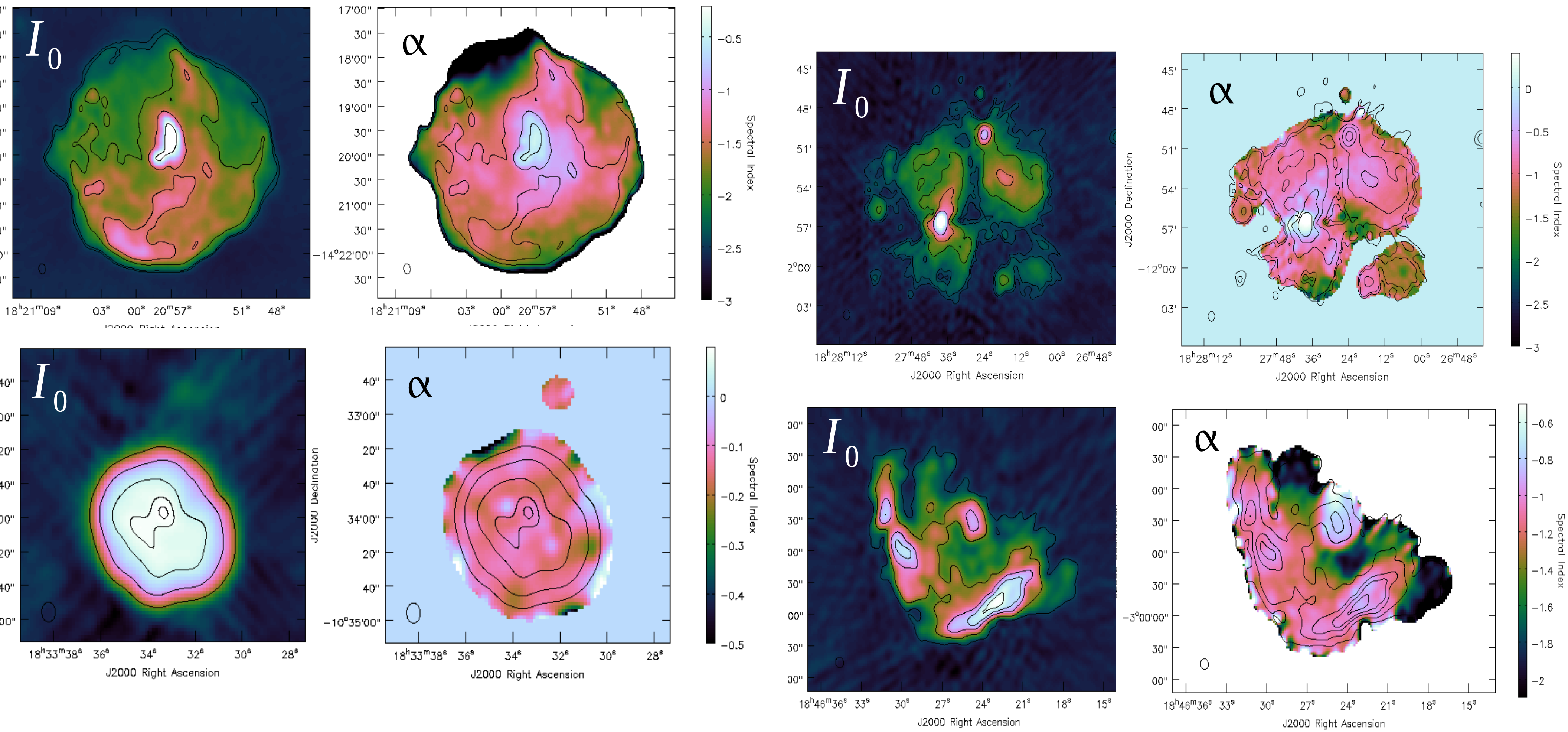

These examples used nterms=2, and about 5 scales.

=> Within 1-2 Ghz and 4-8 GHz, spectral-index error is < 0.2 for SNR>100.

=> Dynamic-range limit of few x 1000 ---> residuals are artifact-dominated

Example : Abell 2256 *[Owen et al, 2014]*

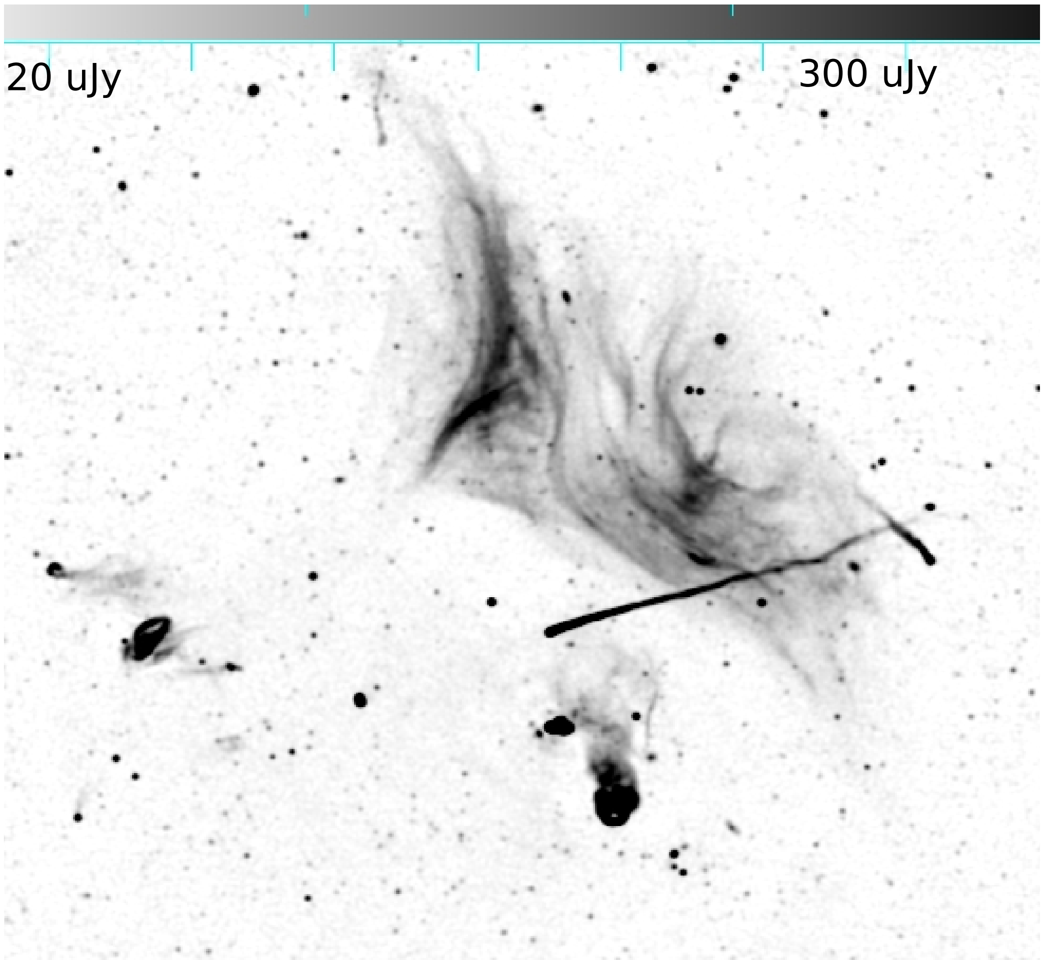

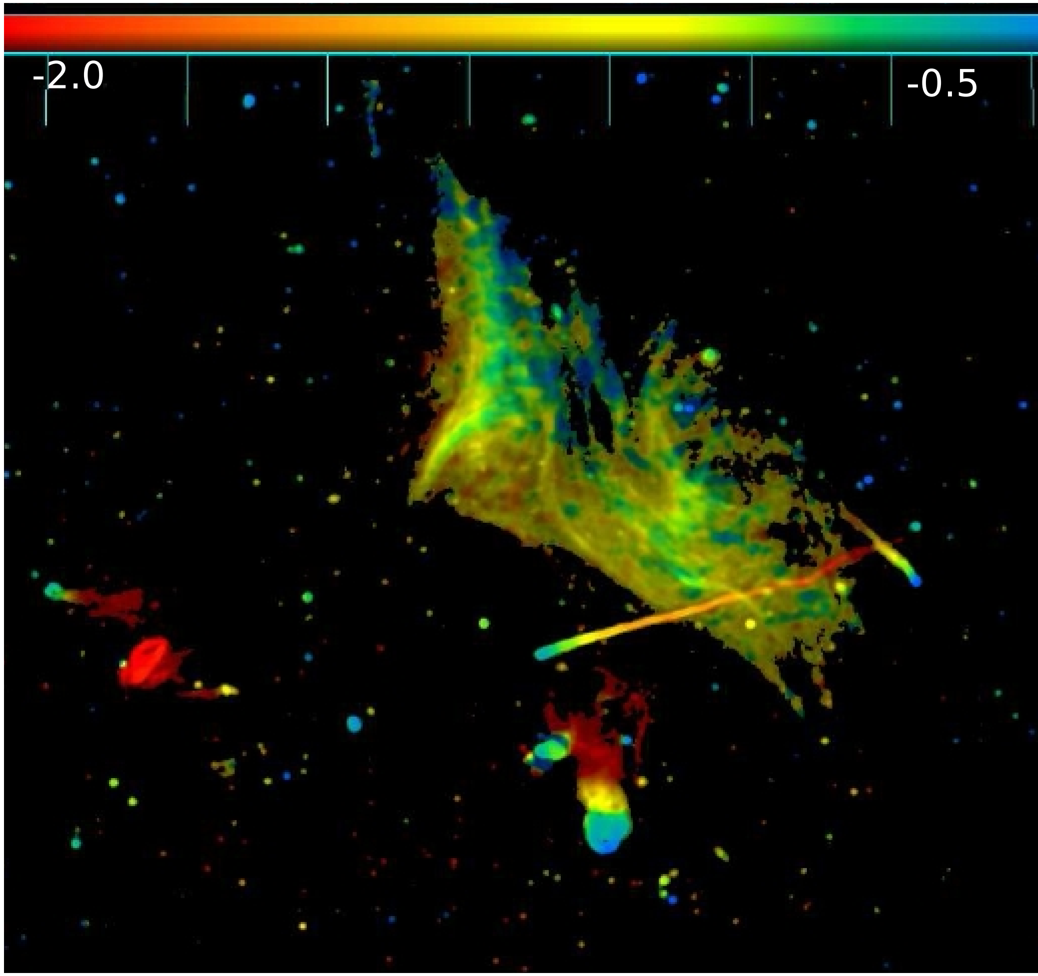

VLA A,B,C,D at L-Band (1-2 GHz), VLA A at S&C bands(2-4, 4-6, 6-8 GHz)

Calibration and Auto-flagging in AIPS. Intensity/Spectral index Imaging in CASA.

Bandwidth smearing (over-averaging in frequency)

Suppose the entire receiver bandwidth was measured in one channel ν_0

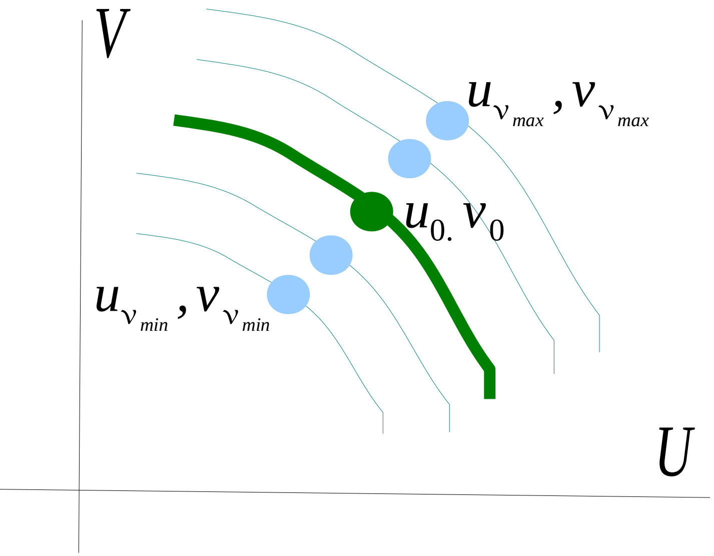

$V(u_\nu)$ is mistakenly mapped to $\frac{\nu_0}{\nu} u_\nu$

Similarity theorem of Fourier-transforms :

Radial shift in source position with frequency.
=> Radial smearing of the sky brightness

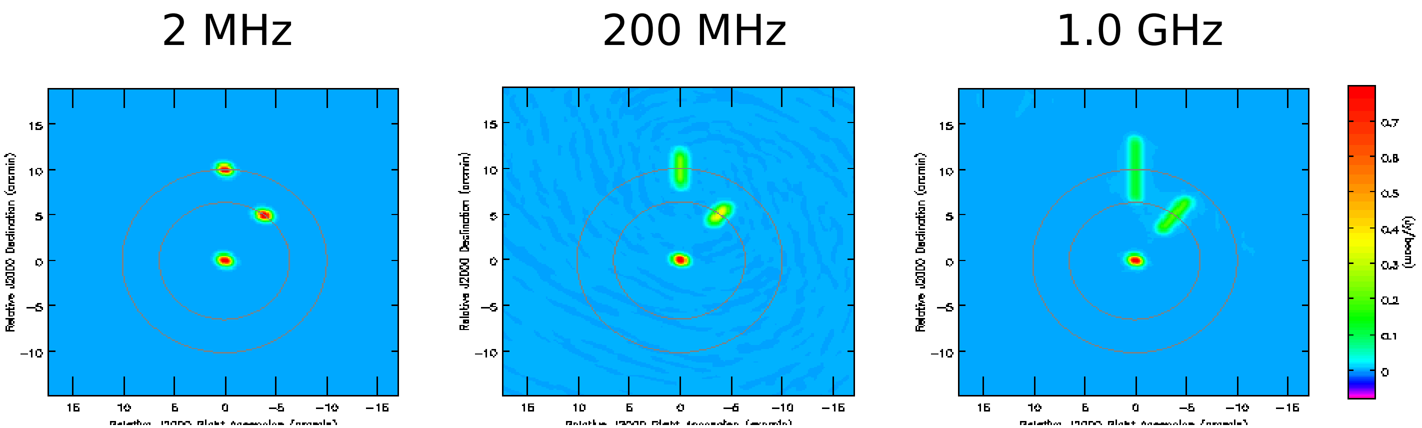

Excessive channel averaging during post-processing has a similar effect.

Bandwidth smearing limit for HPBW field-of-view : $\delta\nu < \frac{\nu_0 D}{b_{max}}$

Bandwidth Smearing limits at L-Band (1.4 GHz),
33 MHz (VLA D-config), 10 MHz (VLA C-config),
3 MHz (VLA B-config), 1 MHz (VLA A-config)

Wide Band

Wide Field

Full Beam

Wide Band + Full Beam

Example : Imaging the G55 supernova remnant

Summary

Wide-Field Imaging – W-term

$$V^{obs}(u,v)=S(u,v)\iiint I(l,m)e^{2\pi i(ul+vm+w(n-1))}\,dl\,dm\,dn$$

w and **n** increase with distance from the image phase center
w increases with baseline length and observing frequency

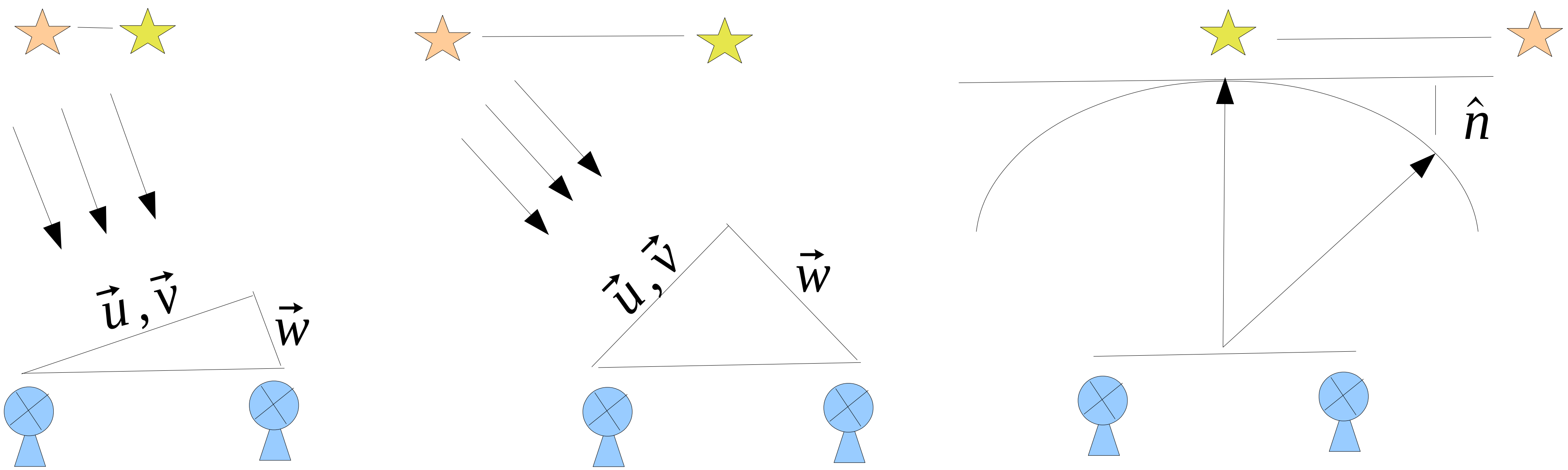

Example : For the VLA, the W-term becomes significant at a radius of

- 1 deg for D-config, L-band (PB : 30arcmin)
- 2 arcmin for A-config, L-band (PB : 30 arcmin)

W-term : Effect on images

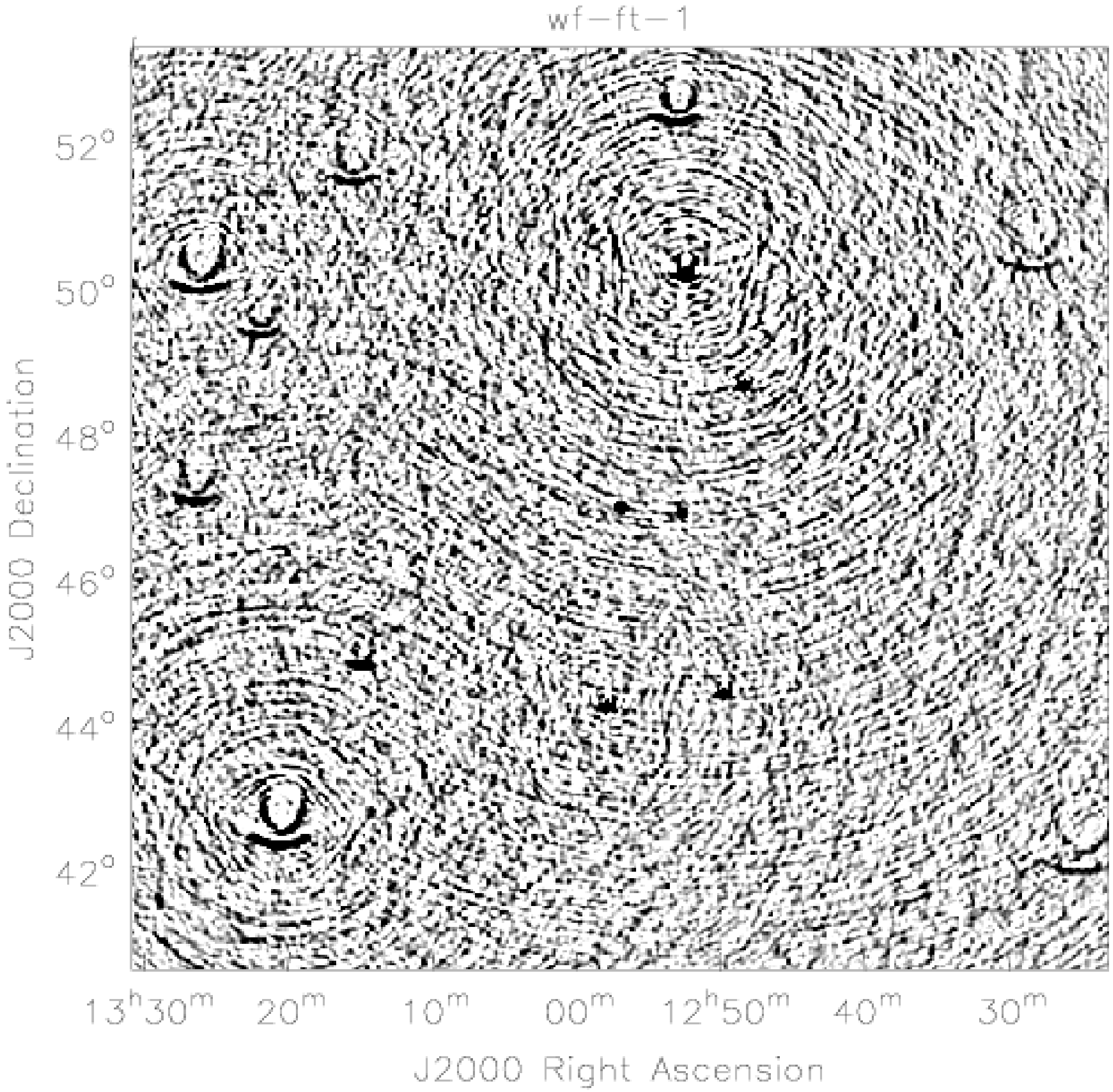

Arcs or shifts for sources away from phase center

W-term is a phase error. Sources move in the image in a systematic way

W-term : Algorithms : Faceting

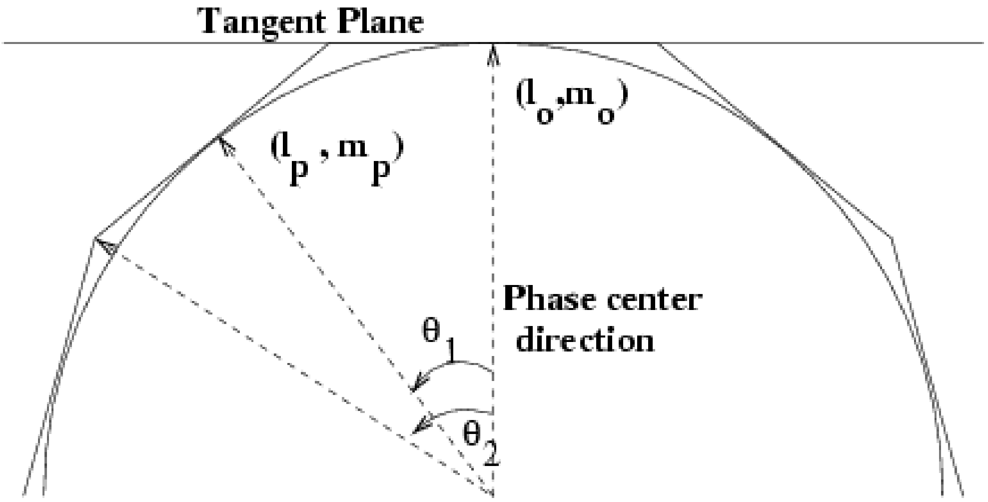

- Approximate the celestial sphere by a set of tangent planes (facets) such that 2D geometry is valid per facet

- Image each facet with its own phase reference center and re-project to the tangent plane

Variants:

Deconvolve facets separately before re-projecting and stitching

(or)

Image all facets onto the same tangent plane grid and perform a joint deconvolution.

Number of facets : $N_{Poly} = \theta_f^2 \frac{B_{max}}{\lambda} max = \frac{B_{max} \lambda_{max}}{[N_{lobes} D]^2}$ $D \equiv Antenna\ diameter;\ \theta_f = Antenna\ FoV$

W-term : Algorithms : W-Projection

For ideal 2D imaging we need to measure E_1'. Instead we measure E_1

E_1' and E_1 are related by a Fresnel diffraction/propagation kernel.

$$G(u,v,w) = FT\left[e^{2\pi\iota w\sqrt{1-l^2-m^2}}\right]$$

$$V^o(u,v,w) = V(u,v,w=0) * G(u,v,w)$$

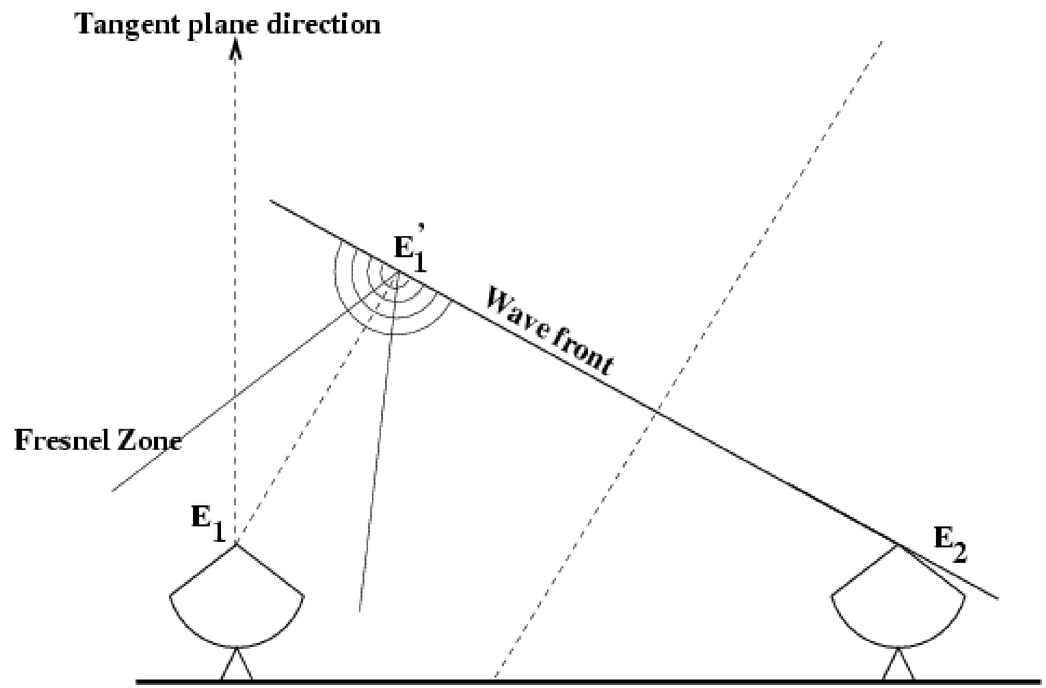

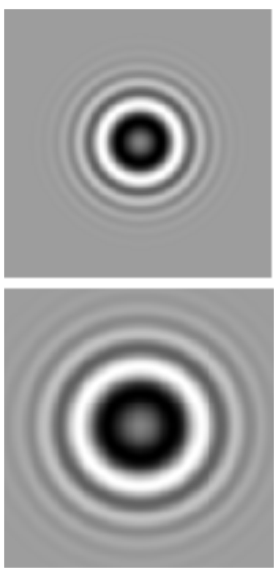

Convolution in uv-domain

=> Correct it by another convolution with the inverse/conjugate kernel (during the gridding step)

=> Use different kernels for different W values (appropriately quantized)

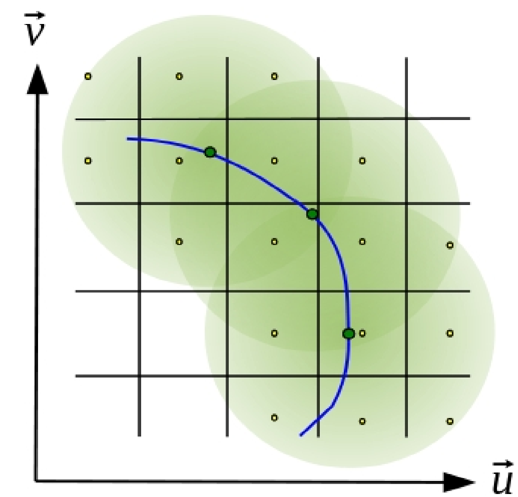

W-term : Example

Cornwell et al, 2008

2D Imaging | Facet Imaging | W-Projection

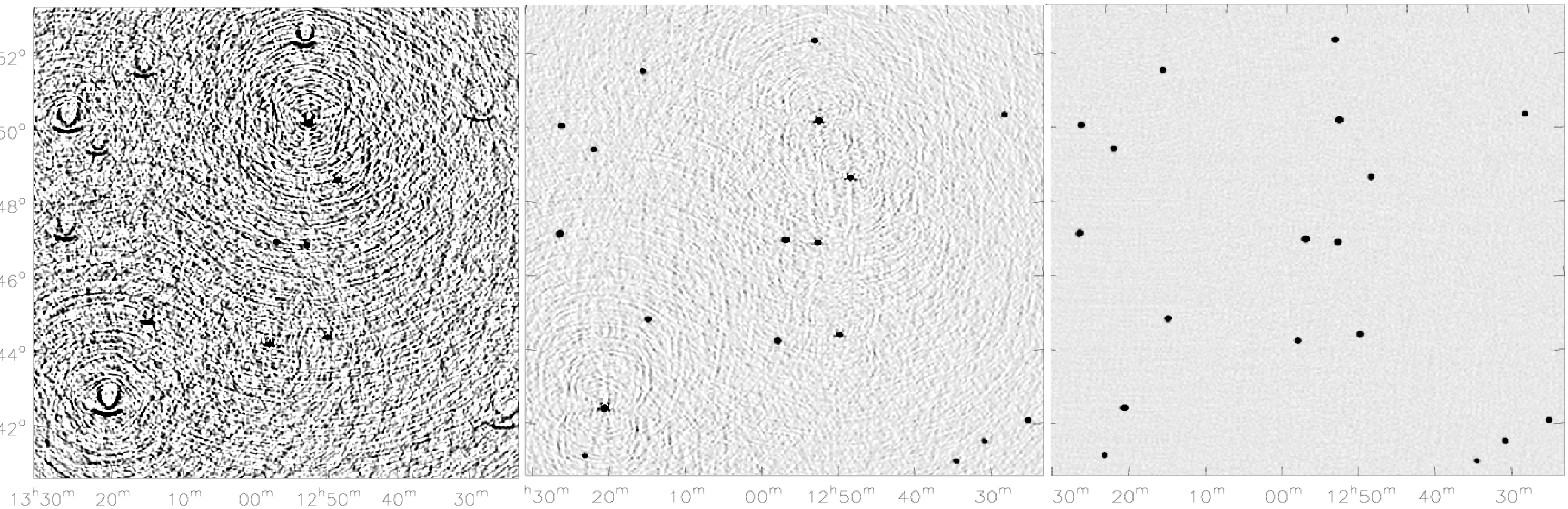

In general, W-Projection is more accurate and faster.

But, for very wide fields of view (such as those offered by dipole arrays), W-Projection kernels may become too large

=> Use a combination of faceting and W-Projection
(or another approach called W-Stacking)

W-term : W-Projection example (74MHz VLA)

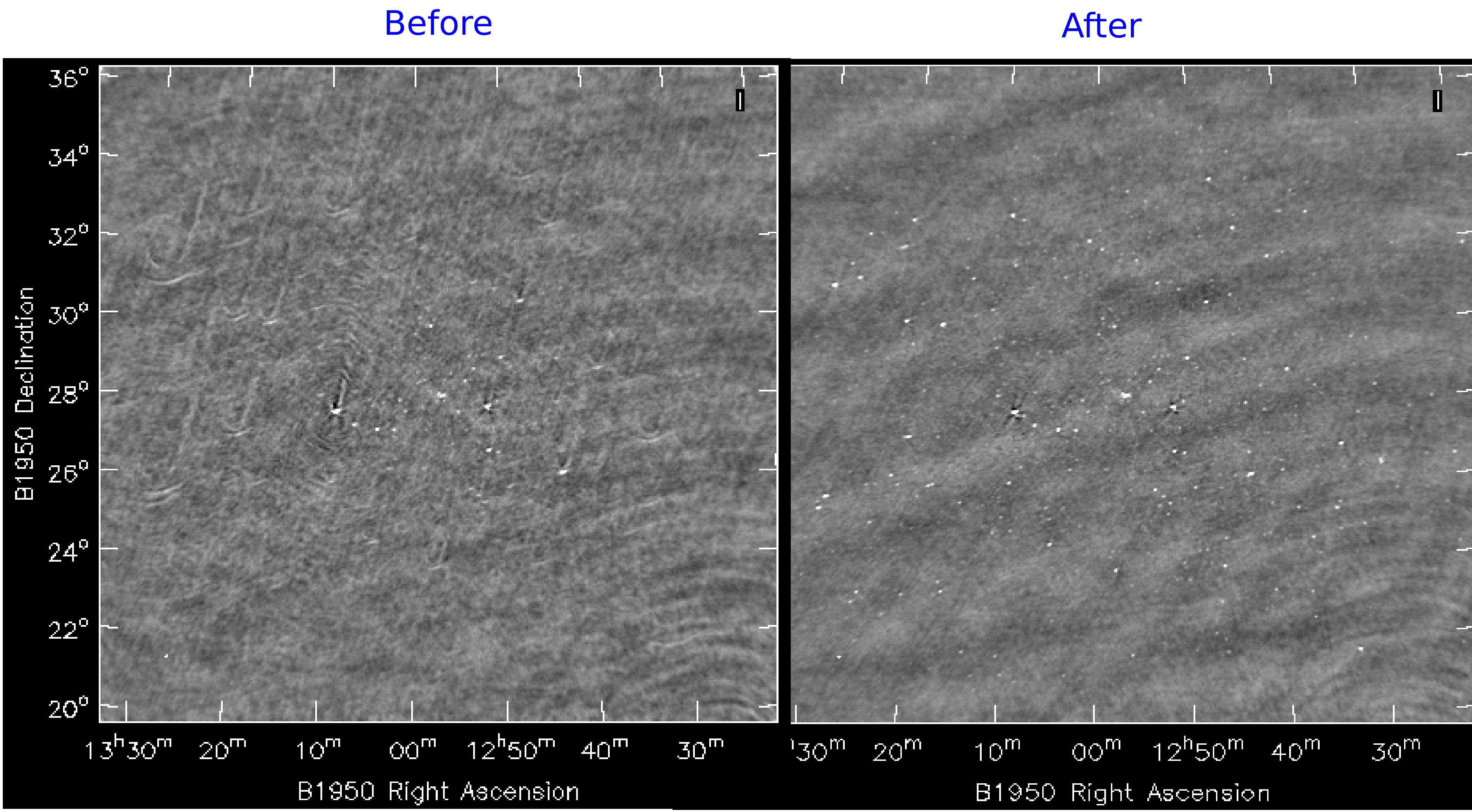

Images from K.Golap

Wide Band

Wide Field

Full Beam

Wide Band + Full Beam

Example : Imaging the G55 supernova remnant

Summary

Wide-Field Imaging – Primary Beams

The Sky is multiplied by a PB, before being sampled by each baseline

$$I^{obs}(l,m) = \sum_{ij,t} I_{ij}^{PSF}(l,m,t) * \left[P_{ij}(l,m,t) \cdot I^{sky}(l,m) \right]$$

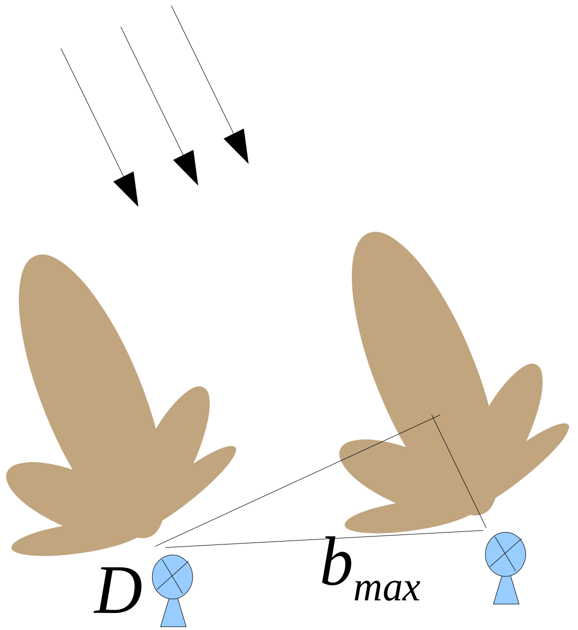

The antenna field of view :
D = antenna diameter

$$\lambda / D$$

Primary Beam
for baseline ij

P_{ij}

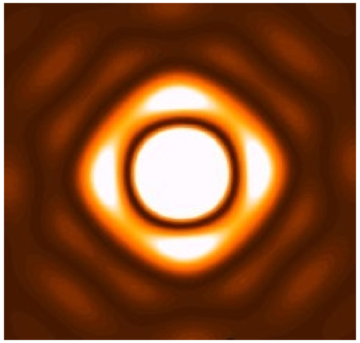

$$P_{ij} = V_i . V_j^* = FT\left[A_i * A_j^* \right] = FT\left[A_{ij} \right]$$

Aperture
Illumination
for antennas
i and j : A_i, A_j

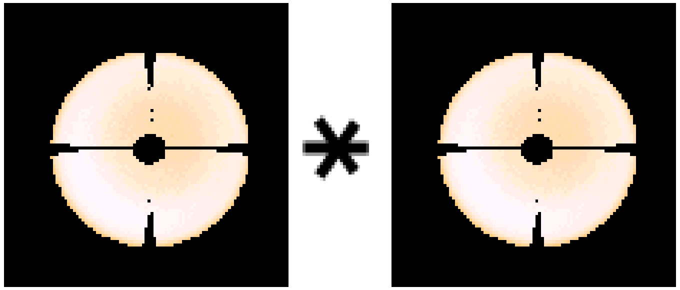

$A_{ij} =$ Baseline aperture Illumination

Primary beams vary within an observation

PB rotates with time, for alt-az mount antennas. (e.g. VLA)

PB varies from antenna to antenna within the array (e.g. ALMA)

PB shape changes with direction on the sky for aperture arrays (e.g. LWA)

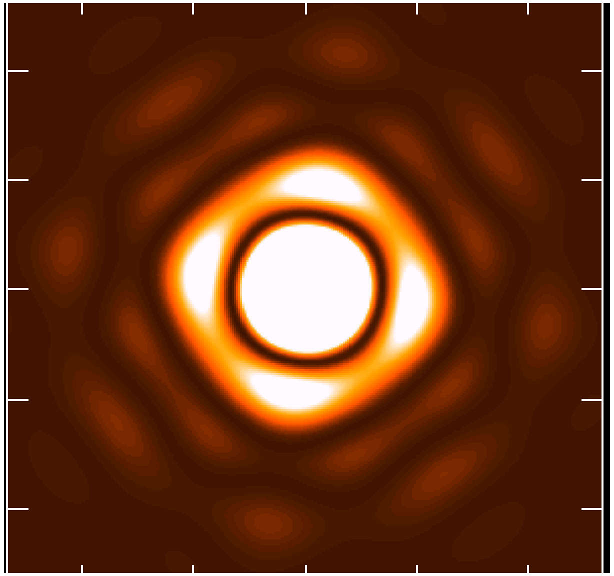

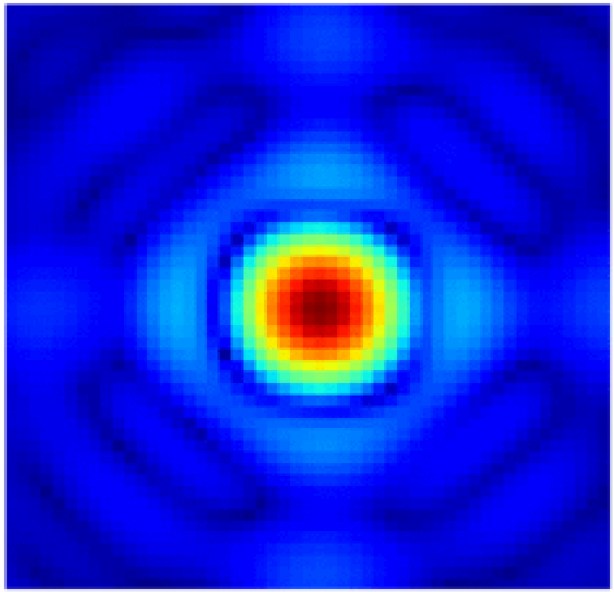

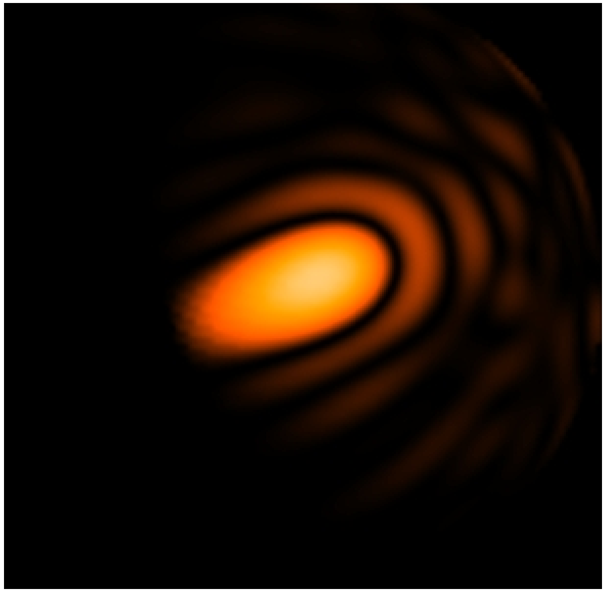

VLA has beam squint

Stokes V

(R – L)

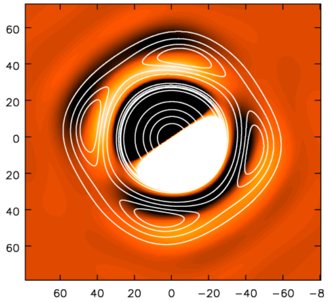

Typically for the ALMA and VLA, errors occur at the 10^4 dynamic range level if such primary beam variations are ignored. Beam squint and pointing offsets cause the dominant errors. For aperture arrays, the shape cannot be ignored.

Primary beams vary within an observation

PB rotates with time, for alt-az mount antennas. (e.g. VLA)

PB varies from antenna to antenna within the array (e.g. ALMA)

PB shape changes with direction on the sky for aperture arrays (e.g. LWA)

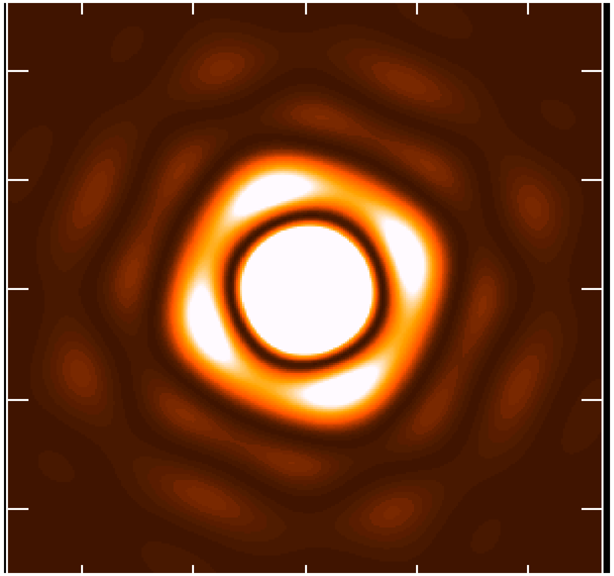

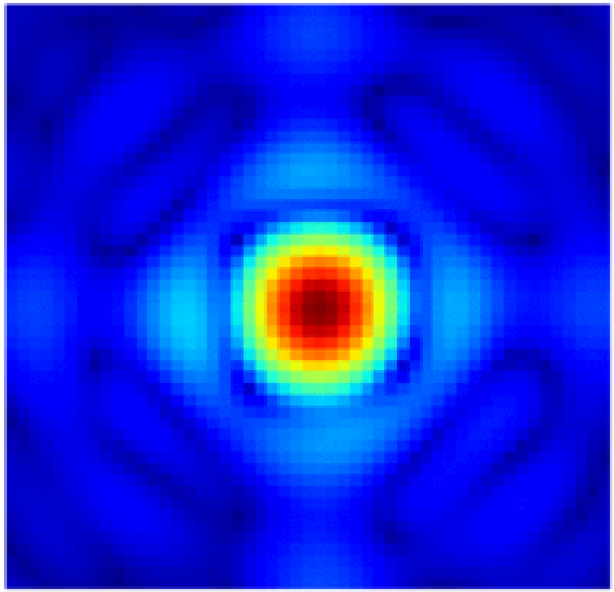

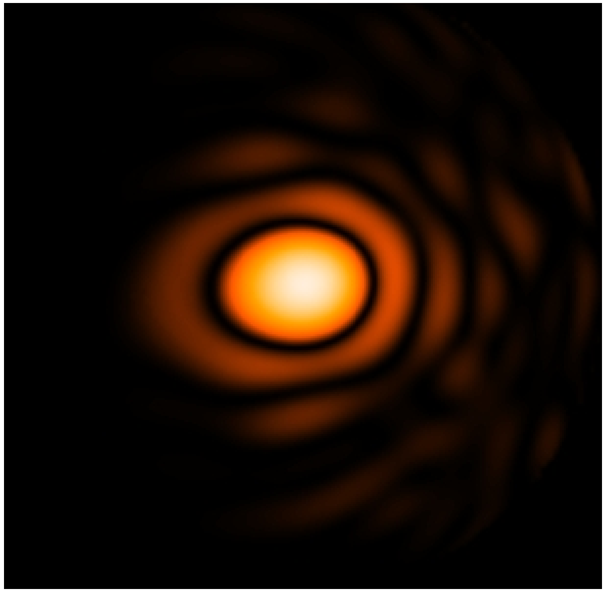

VLA has beam squint

Stokes V

(R – L)

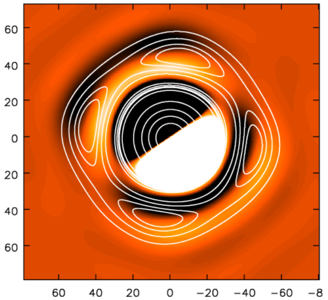

Typically for the ALMA and VLA, errors occur at the 10^4 dynamic range level if such primary beam variations are ignored. Beam squint and pointing offsets cause the dominant errors. For aperture arrays, the shape cannot be ignored.

Primary beams vary within an observation

PB rotates with time, for alt-az mount antennas. (e.g. VLA)

PB varies from antenna to antenna within the array (e.g. ALMA)

PB shape changes with direction on the sky for aperture arrays (e.g. LWA)

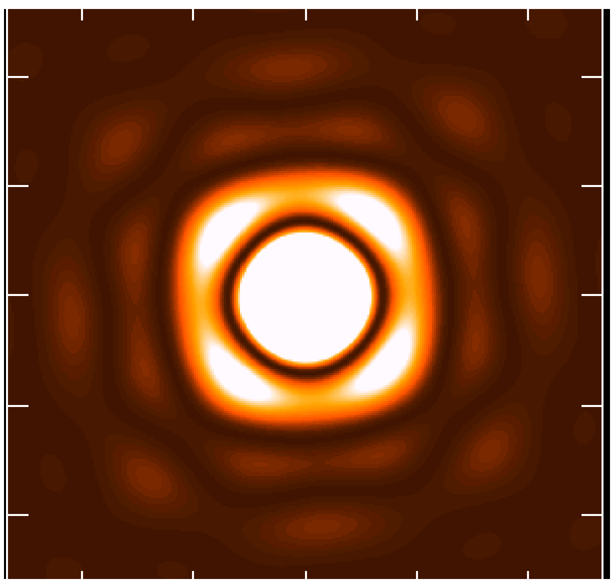

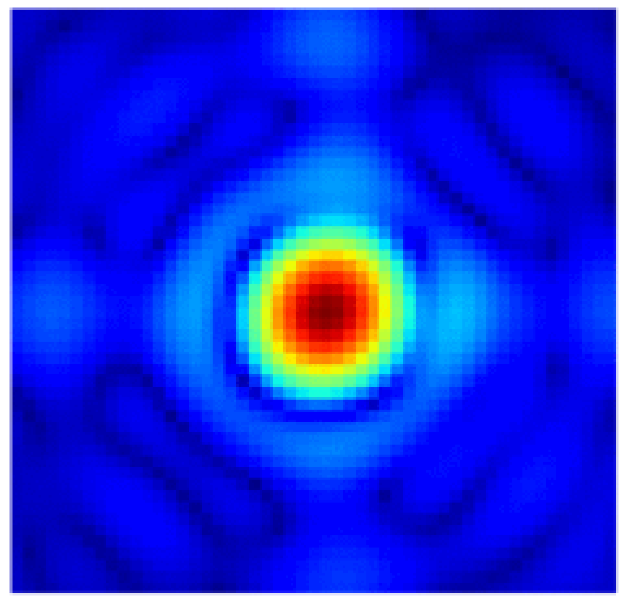

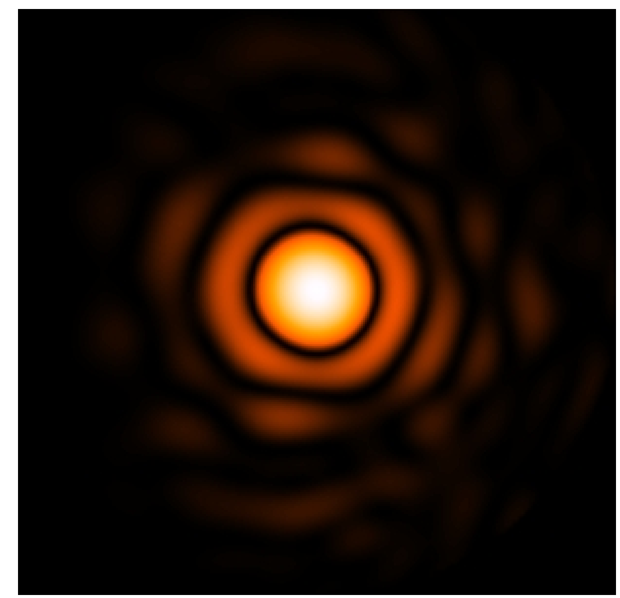

VLA has beam squint

Stokes V

(R – L)

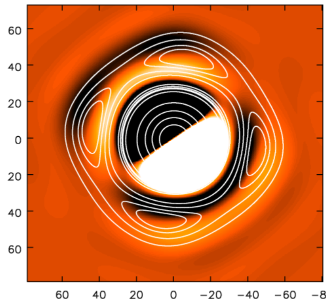

Typically for the ALMA and VLA, errors occur at the 10^4 dynamic range level if such primary beam variations are ignored. Beam squint and pointing offsets cause the dominant errors. For aperture arrays, the shape cannot be ignored.

Primary beams vary within an observation

PB rotates with time, for alt-az mount antennas. (e.g. VLA)

PB varies from antenna to antenna within the array (e.g. ALMA)

PB shape changes with direction on the sky for aperture arrays (e.g. LWA)

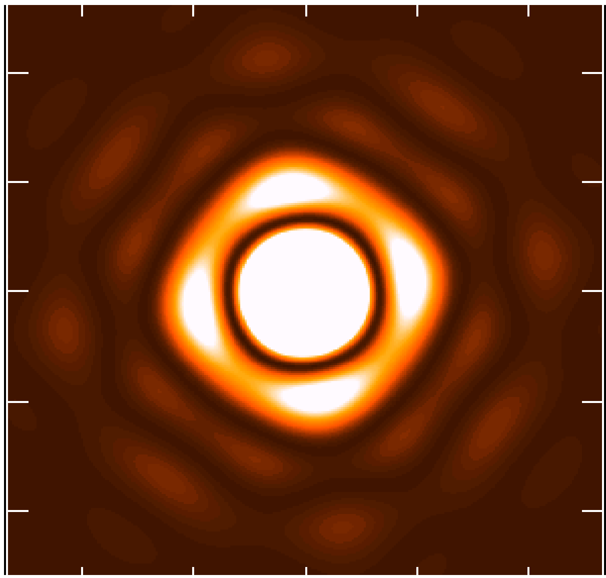

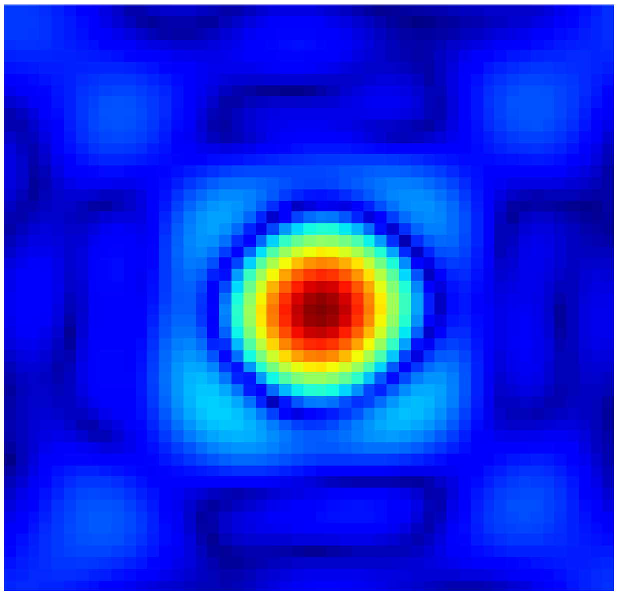

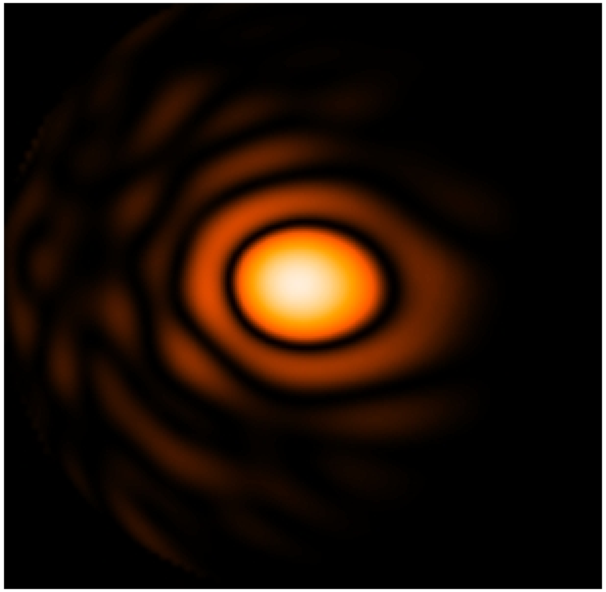

VLA has beam squint

Stokes V

(R – L)

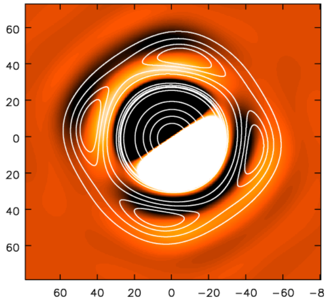

Typically for the ALMA and VLA, errors occur at the 10^4 dynamic range level if such primary beam variations are ignored. Beam squint and pointing offsets cause the dominant errors. For aperture arrays, the shape cannot be ignored.

Primary Beam – Effect on images (VLA simulated example)

(1) Multiplicative gain pattern => attenuation away from the center

(2) Variable gain (due to PB rotation) => artifacts around bright sources.

$$\delta I^{obs} = \sum_t I^{PSF}(t) * \left[\delta P(t) \cdot I^{sky}\right]$$

Dynamic range of 10^4

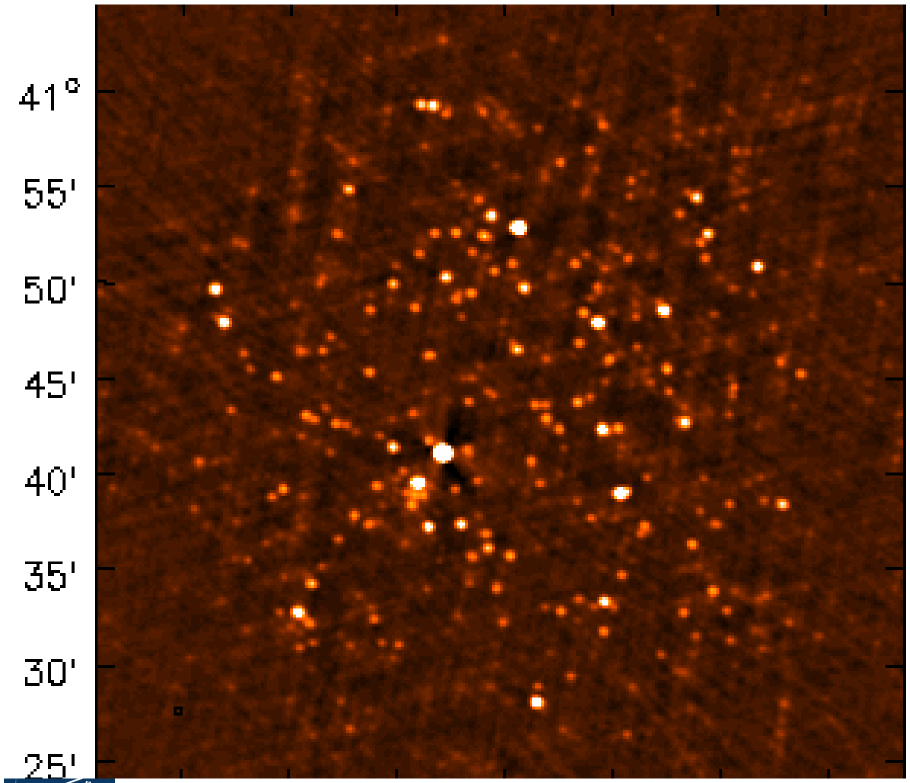

Dynamic range of 10^5

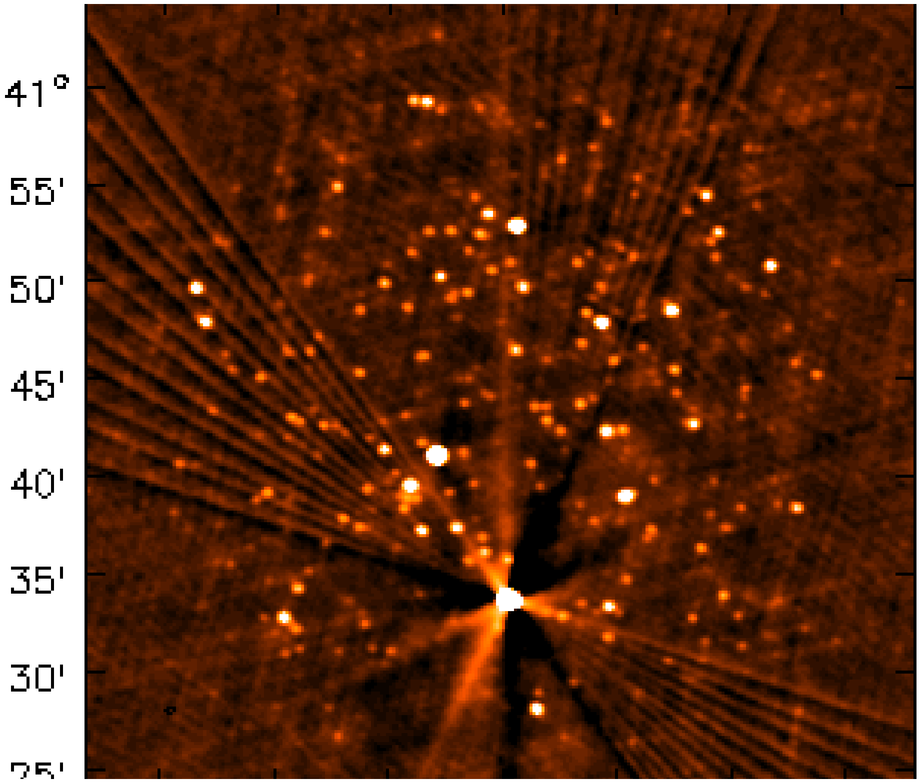

Primary Beam Correction – Post-deconvolution (pbcor)

$$I^{obs}(l,m) \approx I^{PSF}(l,m) * \left[P^{sky}(l,m) \cdot I^{sky}(l,m)\right]$$

Divide out an average primary beam pattern after deconvolution

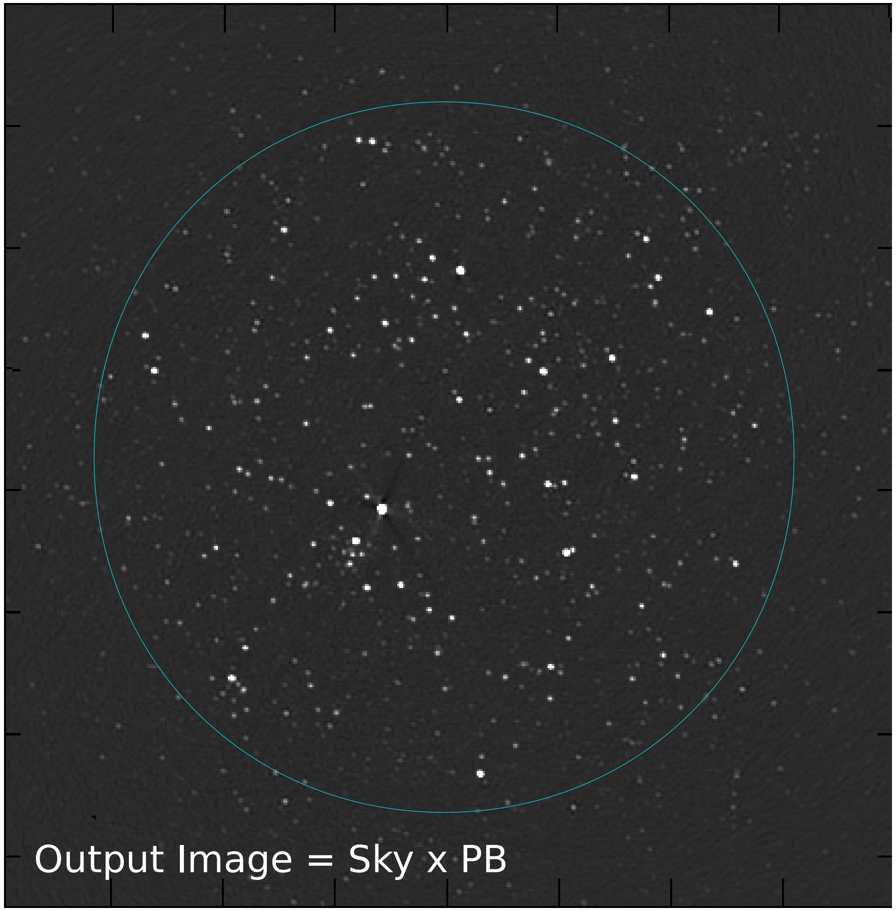

Primary Beam Correction : A-Projection

Bhatnagar et al, 2008

Apply PB correction in the UV-domain **before** visibilities are combined.

$$I_{ij}^{obs} = I_{ij}^{psf} * \left[P_{ij} . I^{sky} \right] \longleftrightarrow V_{ij}^{obs} = S_{ij} . \left[A_{ij} * V^{sky} \right]$$

For each visibility, apply $A_{ij}^{-1} \approx \frac{A_{ij}^{T}}{A_{ij}^{T} * A_{ij}}$

(1) Use A_{ij}^{T} as the convolution function during gridding

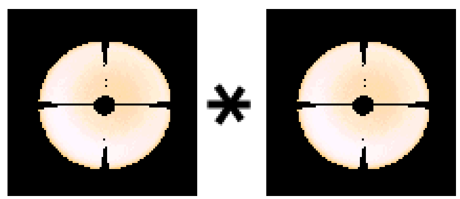

(2) Divide out $FT\left[\sum_{ij} A_{ij}^{T} * A_{ij} \right]$ from the image (in stages).

– Conjugate transpose corrects for known pointing offsets such as beam squint.

– An additional phase ramp is applied for different pointings to make a joint mosaic.

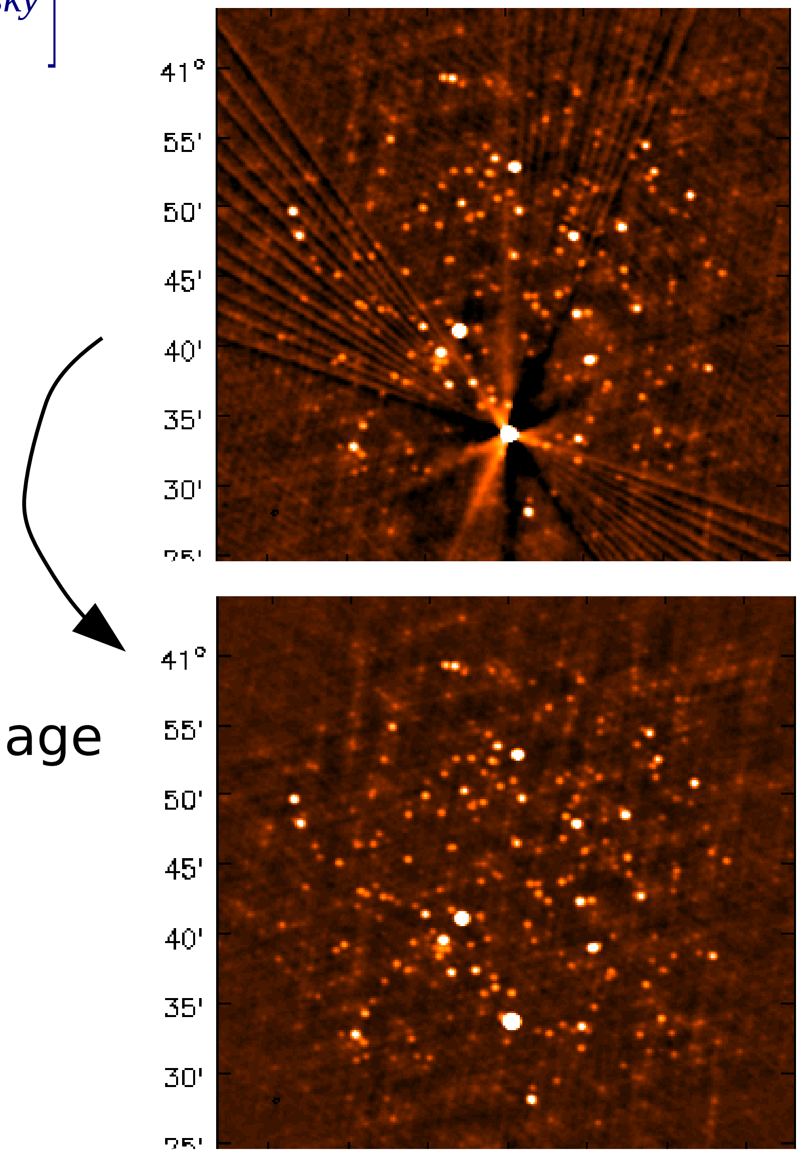

Mueller matrix of the VLA primary beam model

Full polarization primary beams

$P_{ij}^{RR}, P_{ij}^{LL}, etc$

Shows the magnitude of direction dependent polarization leakage

A_{ij}^{T} in A-Projection represents the conjugate transpose of the full matrix

$\left(A_{ij} = FT\left[P_{ij}\right]\right)$

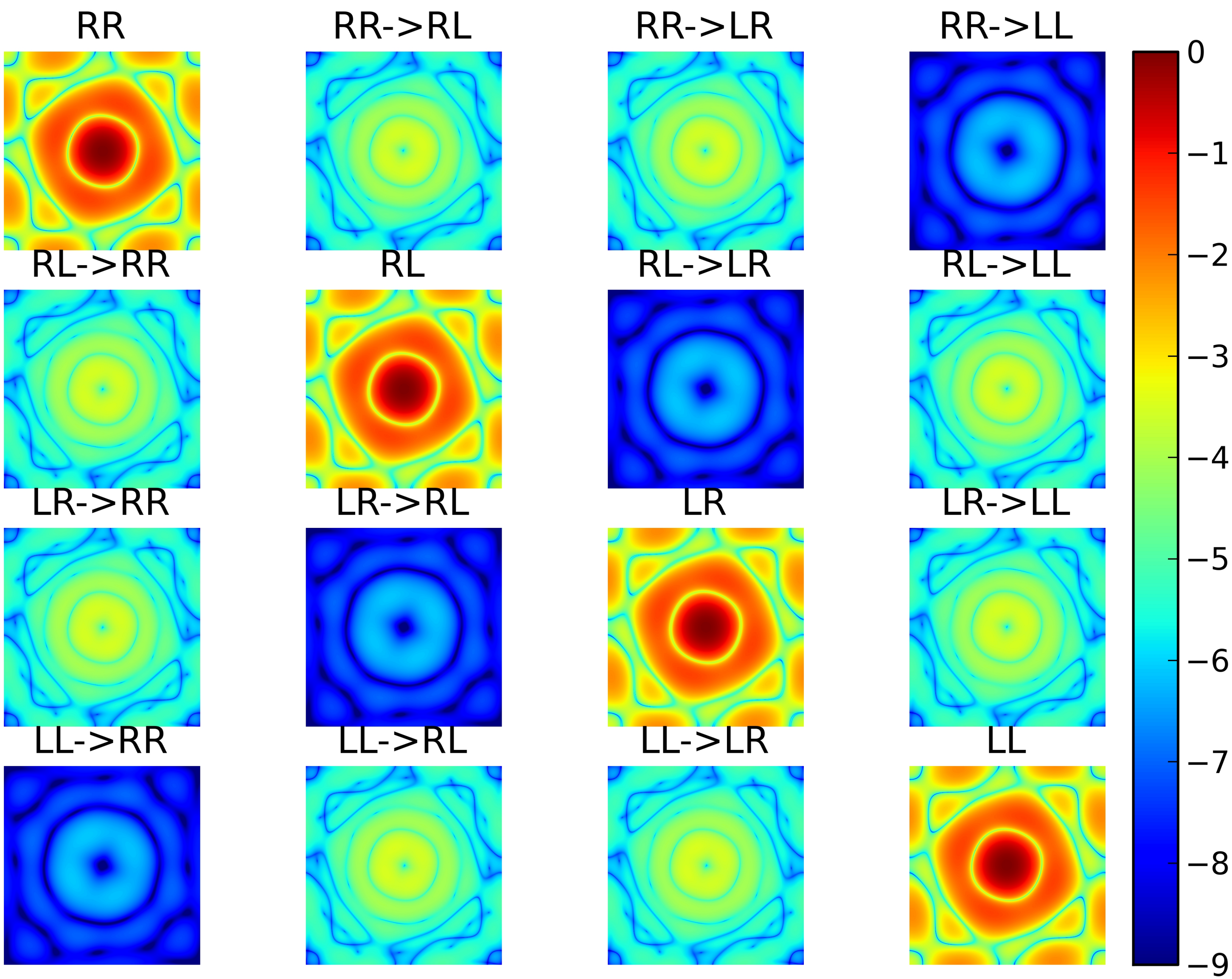

Images from P.Jagannathan

Primary Beam – A-Projection on IC2233 field

Images from S.Bhatnagar

Before

After

Stokes I

Artifacts around all sources away from the pointing center

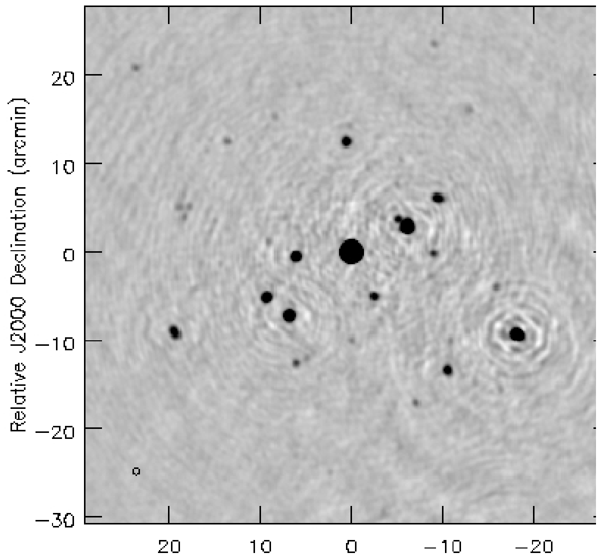

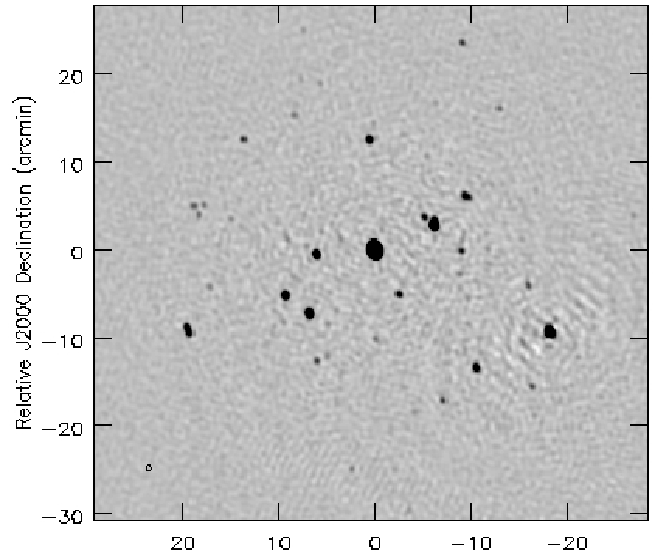

Stokes I

Artifacts removed or reduced within the main lobe

Stokes V

Artificial signals around bright sources due to beam squint

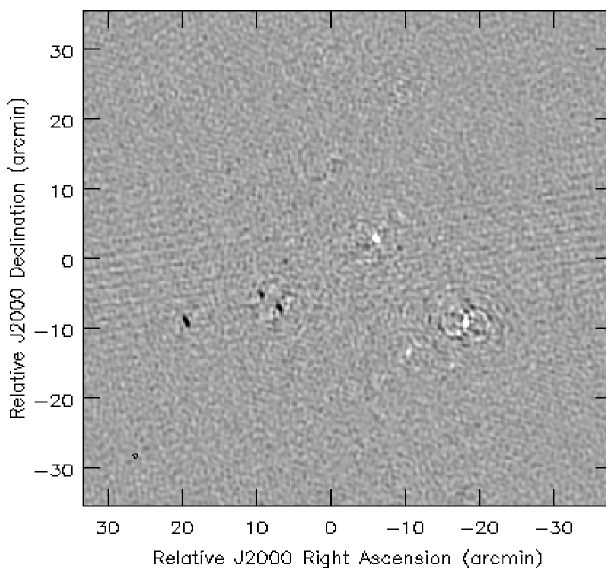

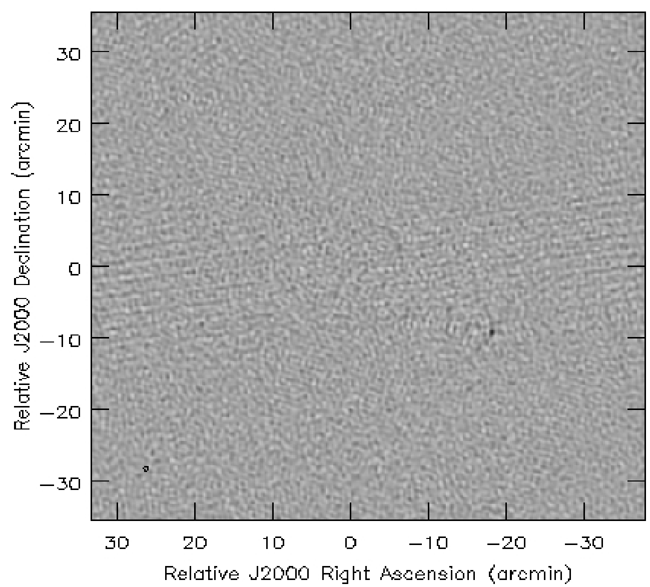

Stokes V

Instrumental Stokes V removed within the main lobe

Accuracy of our PB models outside the main lobe ?

Wide Band

Wide Field

Full Beam

Wide Band + Full Beam

Example : Imaging the G55 supernova remnant

Summary

Wide-Band Wide-Field Imaging : Primary Beams

VLA PBs

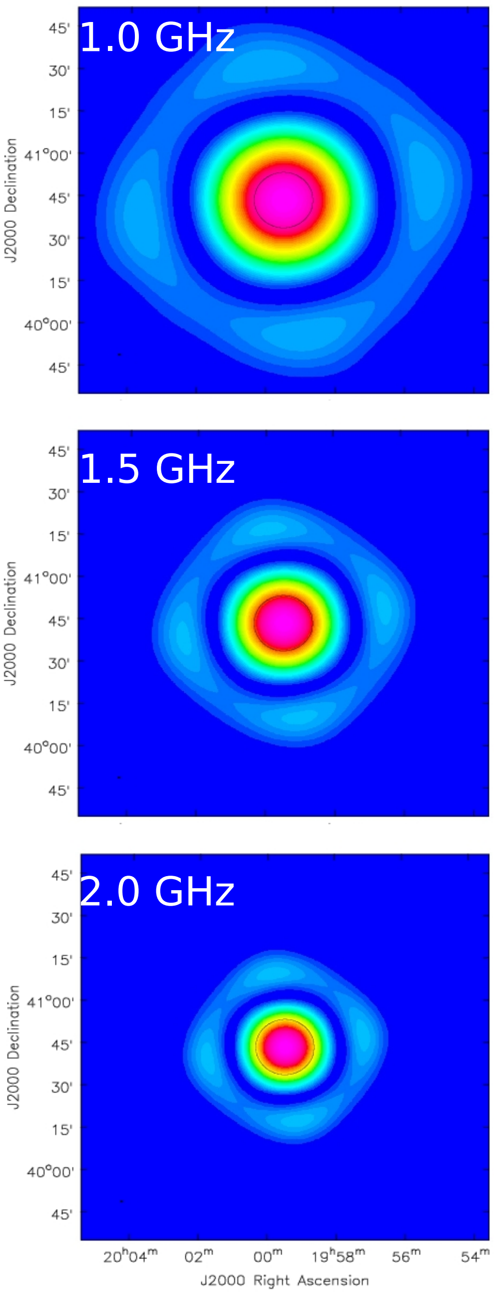

Primary beam size scales with frequency

(PBs also rotate with time and have polarization structure such as beam squint, etc...)

Average Primary Beam

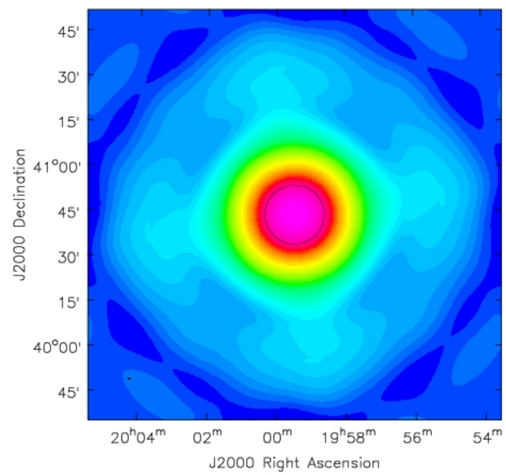

A very wide shelf of sensitivity that extends out to the sidelobes at the lowest frequency.

One channel image : $I_{wf}^{obs} = [P \cdot I^{sky}] * PSF$

Wideband image : $I_{wf,wb}^{obs} = \sum_{\nu} \left[\left(P_{\nu} \cdot I_{\nu}^{sky} \right) * PSF_{\nu} \right]$

Wide-Band Wide-Field Imaging : Primary Beams

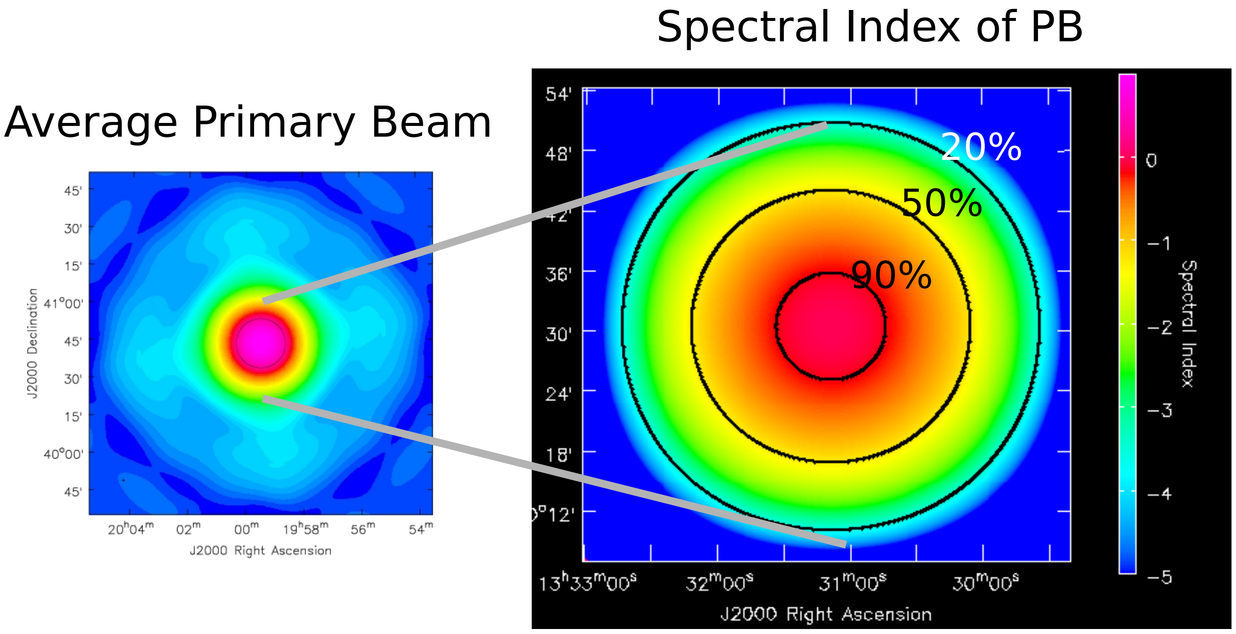

MFS : artificial 'spectral index' away from the center

For VLA L-Band (1-2 GHz)

- About -0.4 at the PB=0.8
  (6 arcmin from the center)

- About -1.4 at the HPBW
  (15 arcmin from the center)

A mosaic primary beam has an artificial spectral index all over.

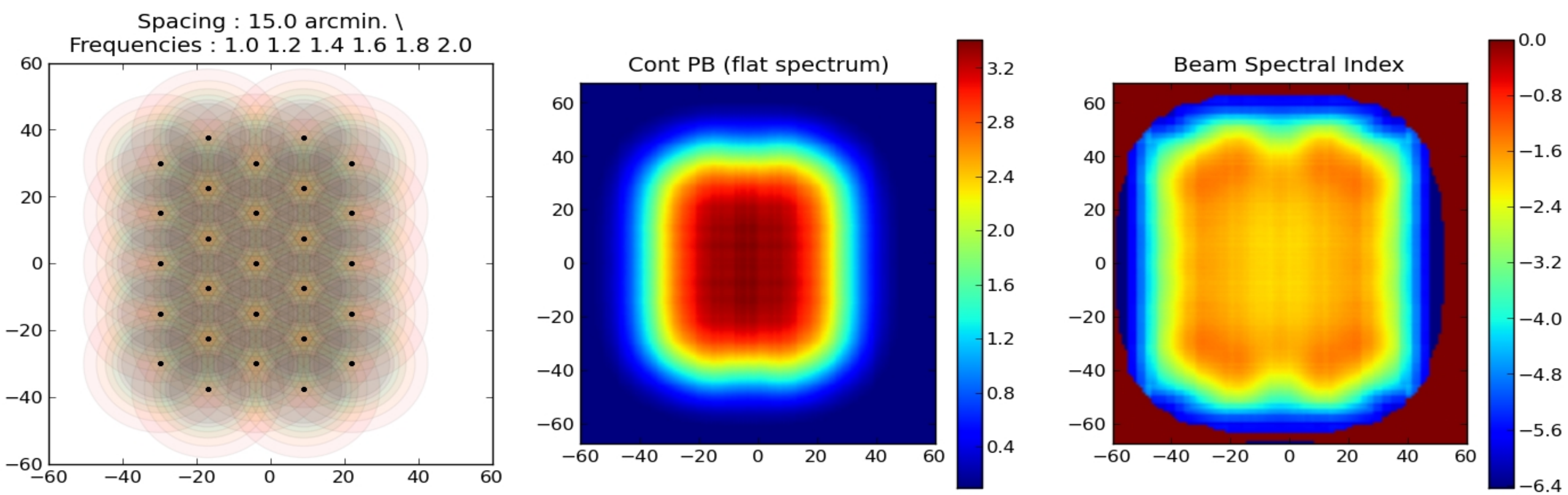

Wide-Band Primary Beam Correction

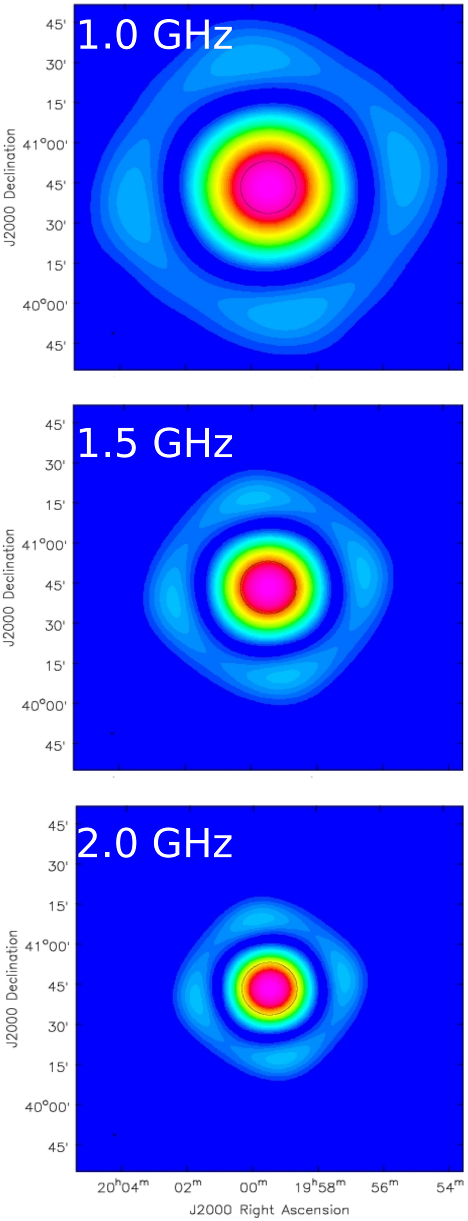

Cube Imaging

-- Sky model represents $I(\nu)P(\nu)$
-- Divide the output image at each frequency by $P(\nu)$

Multi-Term MFS Imaging

-- Taylor coefficients represent $I(\nu)P(\nu)$

-- Polynomial division by PB Taylor coefficients

$$\frac{(I_{0,}^{m} I_{1,}^{m} I_{2,}^{m} \ldots)}{(P_{0,} P_{1,} P_{2,} \ldots)} = (I_{0,}^{sky} I_{1,}^{sky} I_{2}^{sky} \ldots)$$

Wideband A-Projection

-- Remove $P(\nu)$ during gridding (before model fitting) while handling PB rotation/squint

$$A_{\nu}^{-1} \approx \frac{A_{\nu_c}^{T}}{A_{\nu_c}^{T} * A_{\nu}} \quad \text{where} \quad P_{\nu} . P_{\nu_c} \approx P_{\nu_{mid}}^{2}$$

-- Output spectral index image represents only the sky

Bhatnagar et al, 2013

Wideband VLA imaging of IC10 Dwarf Galaxy *[Heesen et al, 2011]*

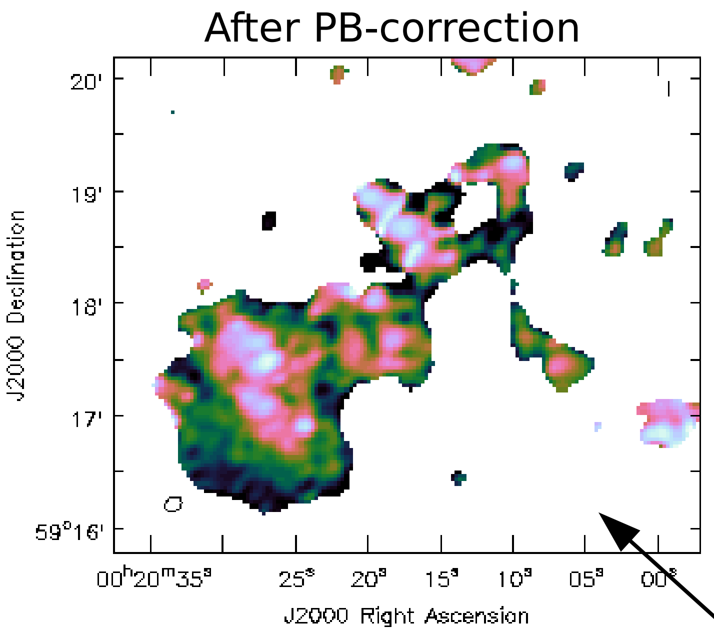

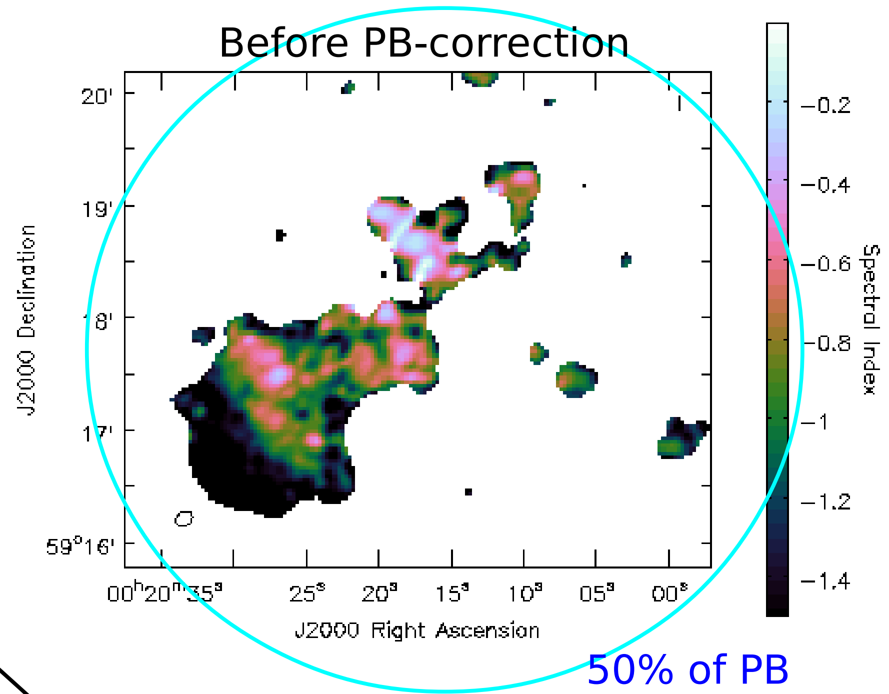

IC10 Dwarf Galaxy :

Spectral Index across C-Band.

Dynamic-range ~ 2000

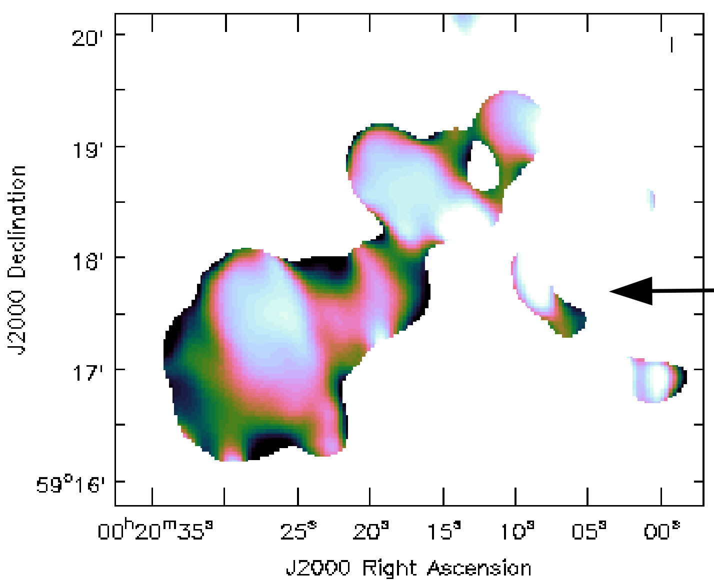

MT-MFS : Wide-band PB-correction after multi-term multi-scale MFS.

Cube : Spectral-index map made by cube imaging, smoothing to lowest resolution, and spectral fitting.

Wide Band Full Beam imaging – Different algorithms

Basic MFS imaging

(no WB,WF corrections)

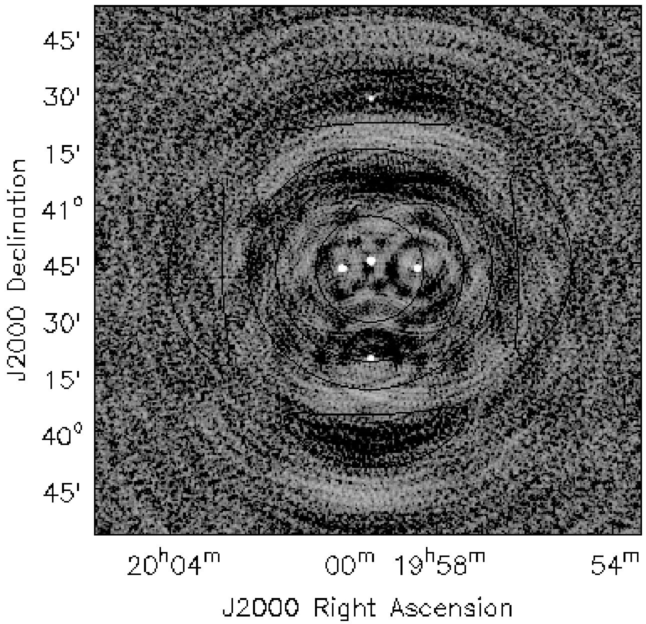

MT-MFS wideband imaging

(No WF corrections, PB freq dependence part of sky model)

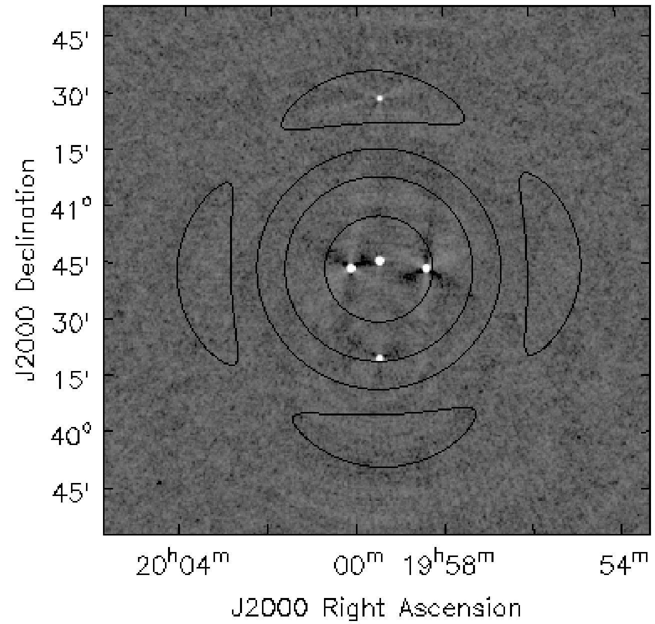

MT-MFS wideband imaging + A-Proj

(PB^2 freq dependence part of sky model)

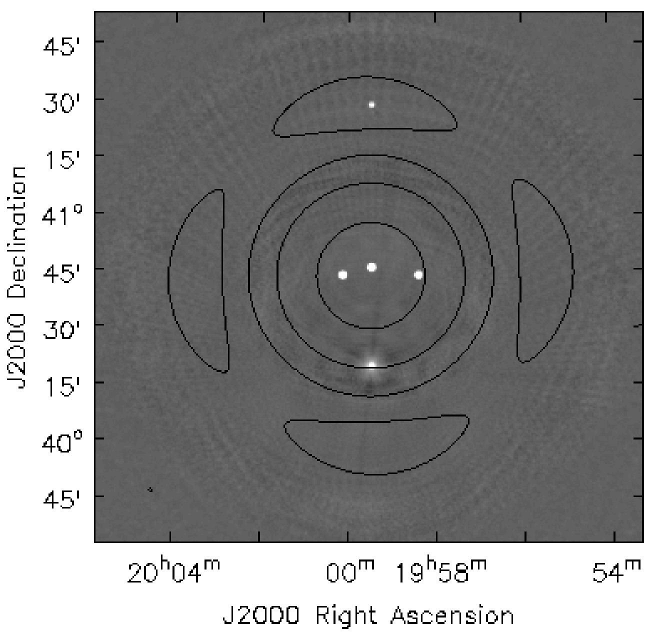

MT-MFS wideband imaging + WB-A-Proj

(PB freq dependence removed during gridding)

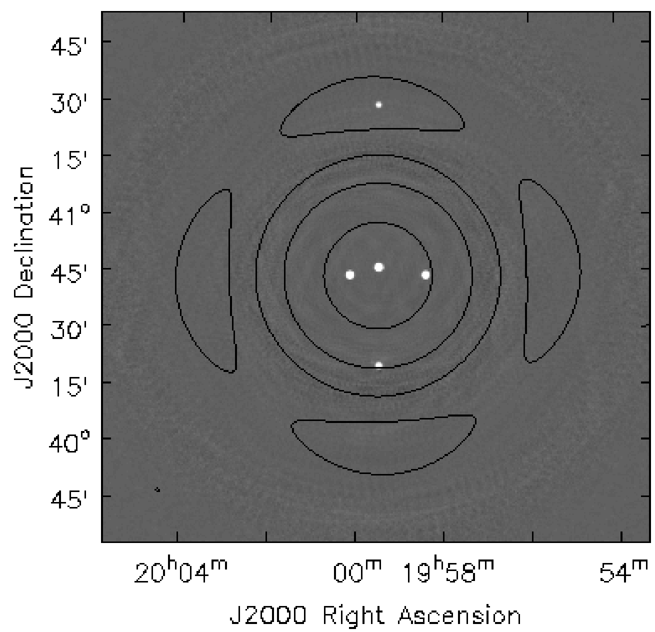

Wideband Mosaic of CTB80 (1-2 GHz, VLA-D config)

Intensity

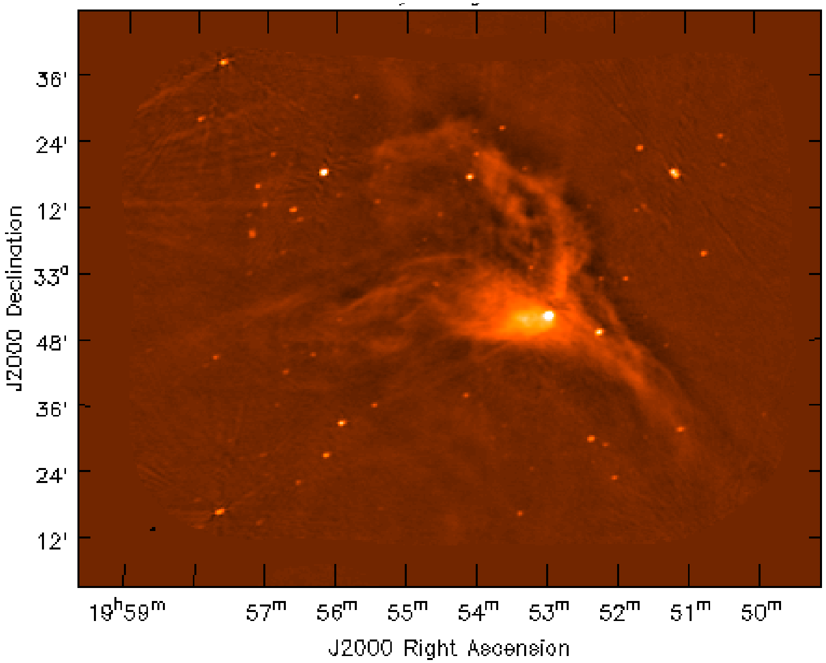

Mosaic Primary Beam

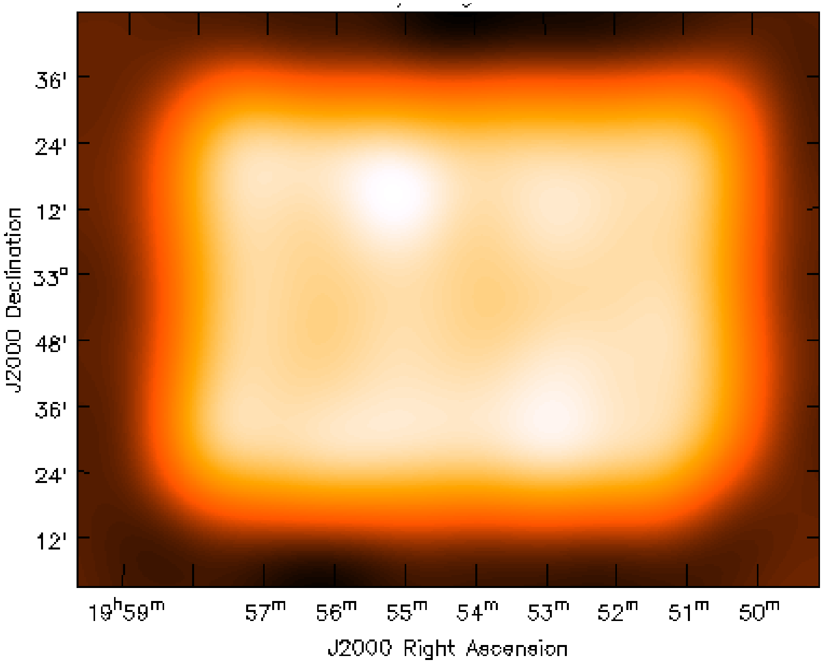

Intensity-weighted
Spectral Index

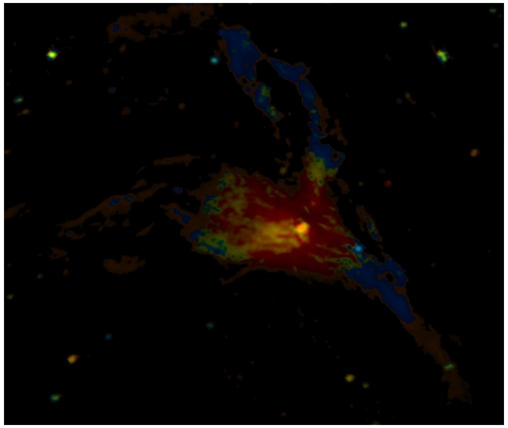

300GB calibrated dataset, 106 pointings over 1.5x2 deg, imaged with MT-MFS (NT=2) and WB-A-Projection.

Major cycle runtime without parallelization : ~10 days.
With 40 processes : 5 hrs (CASA)

Wide Band

Wide Field

Full Beam

Wide Band + Full Beam

Example : Imaging the G55 supernova remnant

Summary

Example : SNR G55.7+3.4

7 hour synthesis, L-Band, 8 spws x 64 chans x 2 MHz, 1sec integrations

Due to RFI, only 4 SPWs were initially imaged (1256, 1384, 1648, 1776 MHz)

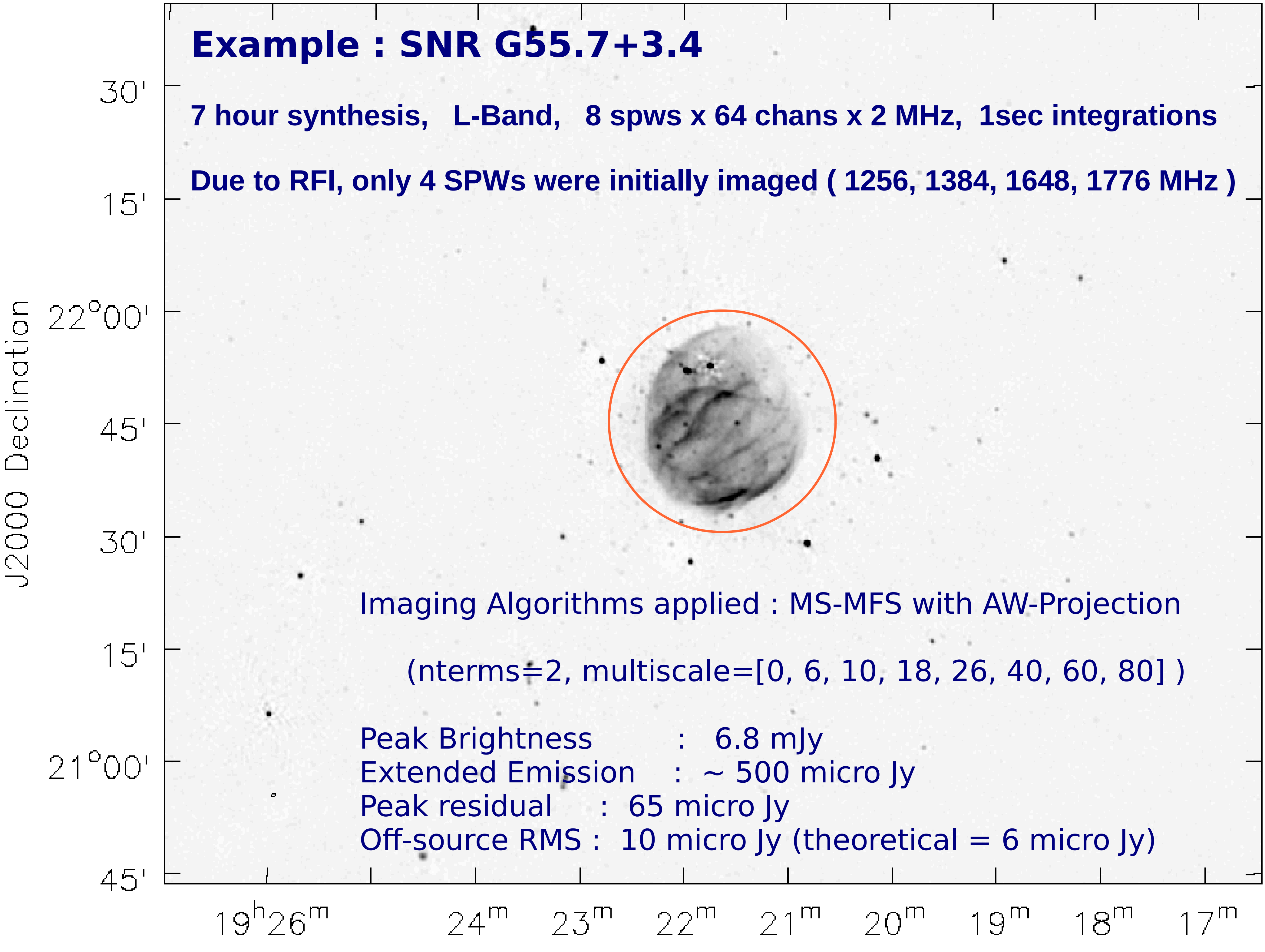

Imaging Algorithms applied : MS-MFS with AW-Projection

(nterms=2, multiscale=[0, 6, 10, 18, 26, 40, 60, 80])

Peak Brightness : 6.8 mJy
Extended Emission : ~ 500 micro Jy
Peak residual : 65 micro Jy
Off-source RMS : 10 micro Jy (theoretical = 6 micro Jy)

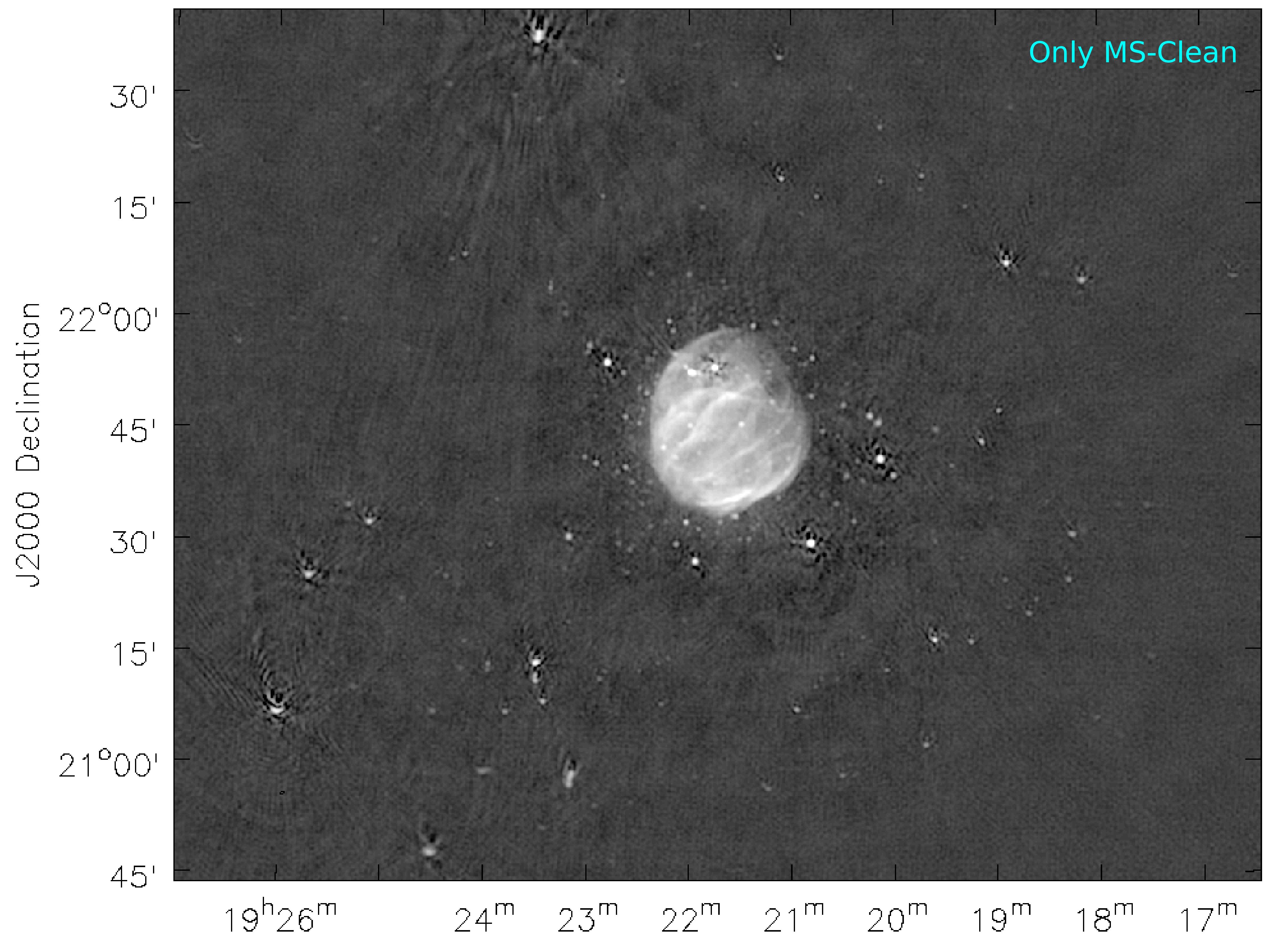

Only MS-Clean
30'
15'
22°00'
45'
30'
15'
21°00'
45'
J2000 Declination
19h26m
24m
23m
22m
21m
20m
19m
18m
17m

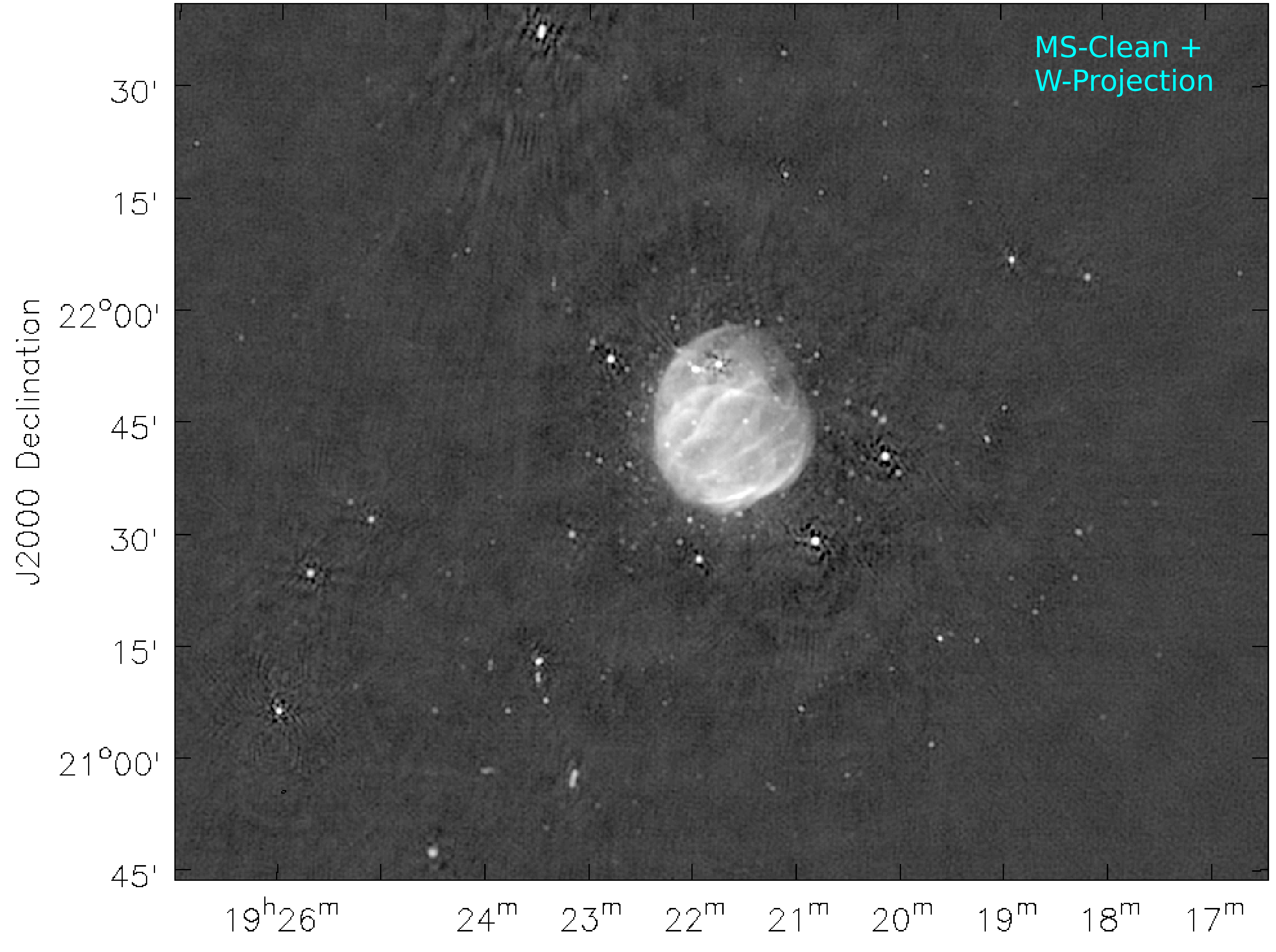
MS-Clean +
W-Projection
J2000 Declination
30'
15'
22°00'
45'
30'
15'
21°00'
45'
19h26m
24m
23m
22m
21m
20m
19m
18m
17m

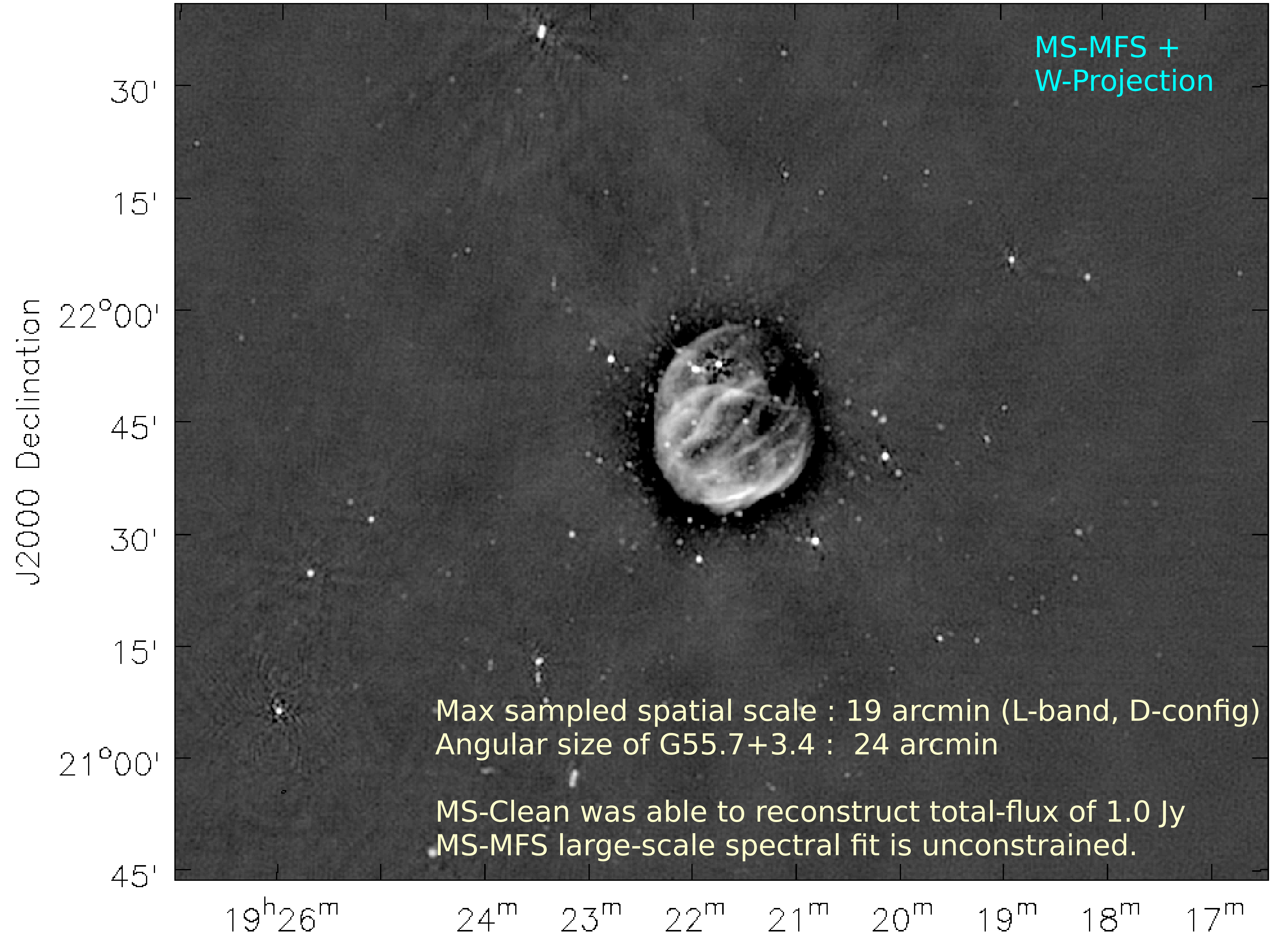
MS-MFS +
W-Projection
J2000 Declination
30'
15'
22°00'
45'
30'
15'
21°00'
45'
19h26m
24m
23m
22m
21m
20m
19m
18m
17m
Max sampled spatial scale : 19 arcmin (L-band, D-config)
Angular size of G55.7+3.4 : 24 arcmin
MS-Clean was able to reconstruct total-flux of 1.0 Jy
MS-MFS large-scale spectral fit is unconstrained.

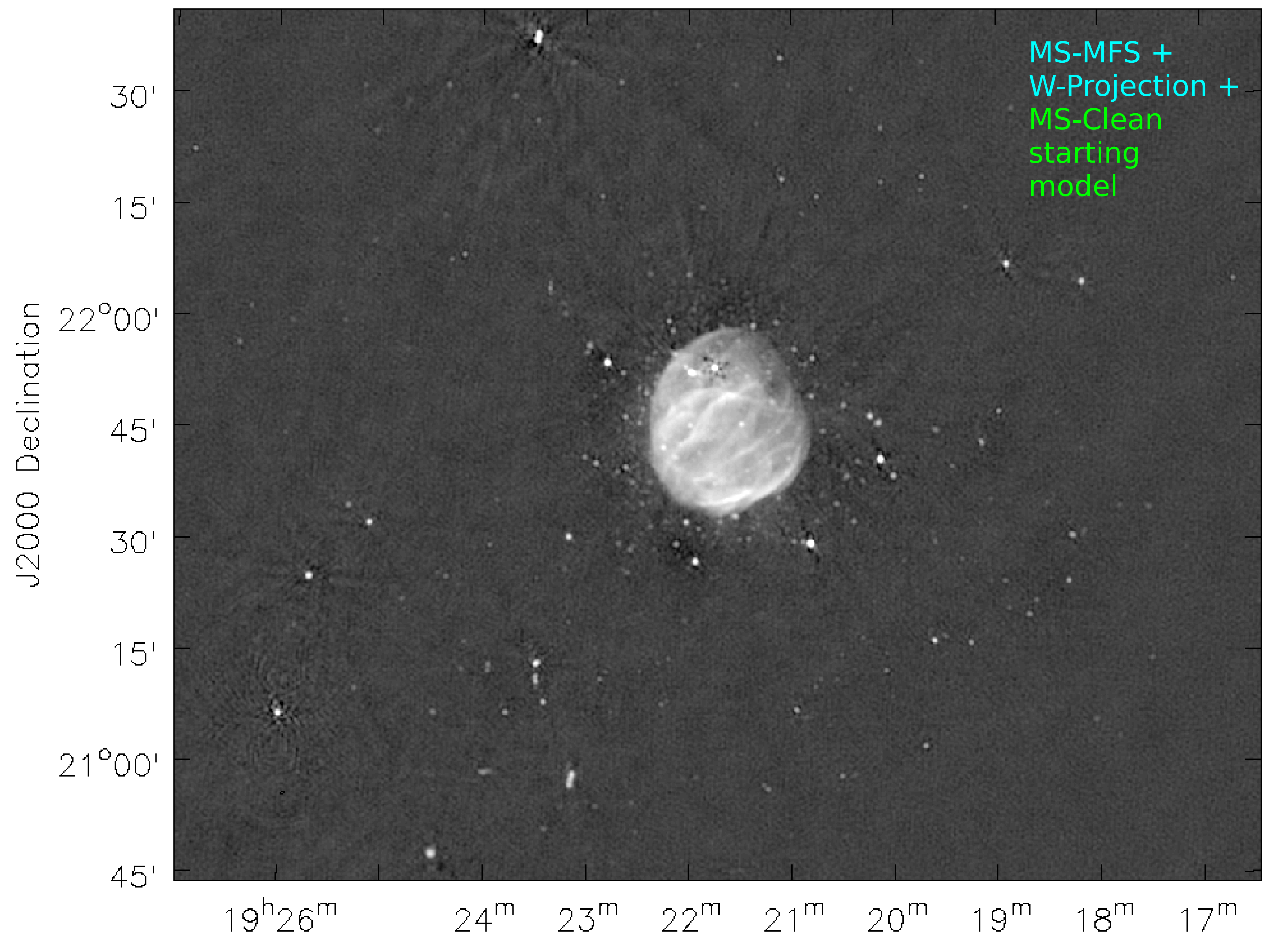
MS-MFS +
W-Projection +
MS-Clean
starting
model
J2000 Declination
30'
15'
22°00'
45'
30'
15'
21°00'
45'
19h26m
24m
23m
22m
21m
20m
19m
18m
17m

Spectral Indices before and after WB-A-Projection

Without PB correction
Outer sources are artificially steep

With PB correction (via WB-AWP)
Outer sources have correct spectra

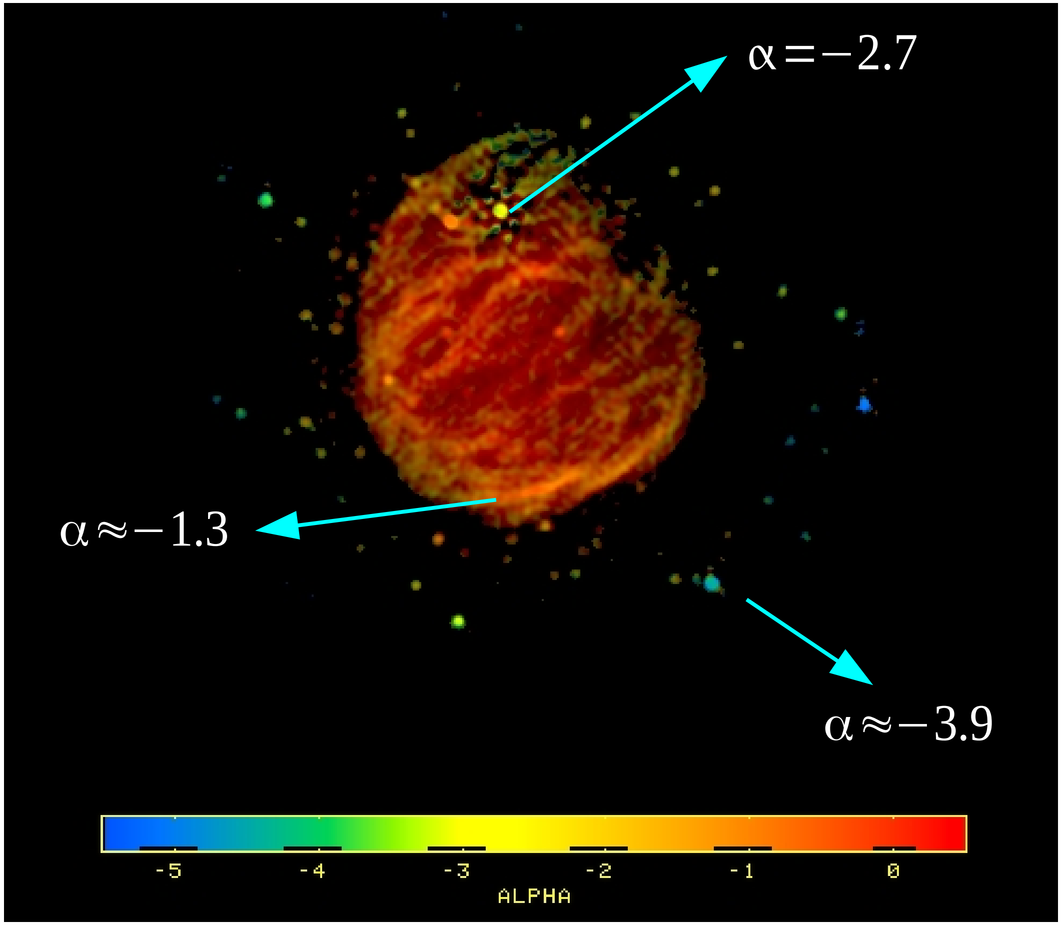

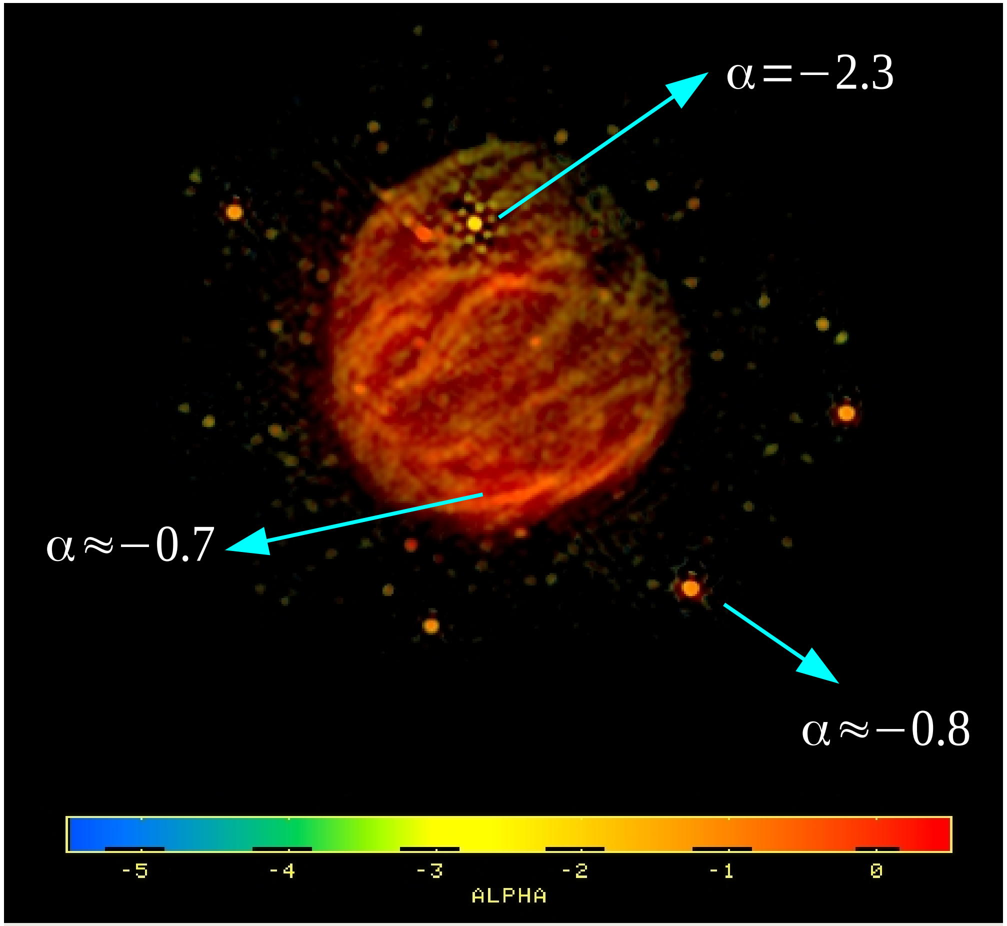

Intensity-weighted spectral index maps (color = spectral index from -5.0 to +0.2)

Wide-field sensitivity because of wide-bandwidths

G55.7+3.4 : Field-of-view of 4x4 degrees from one EVLA pointing at 1-2 GHz

1 Jy total flux

24 arcmin

(PB: 30 arcmin)

10 micro Jy RMS

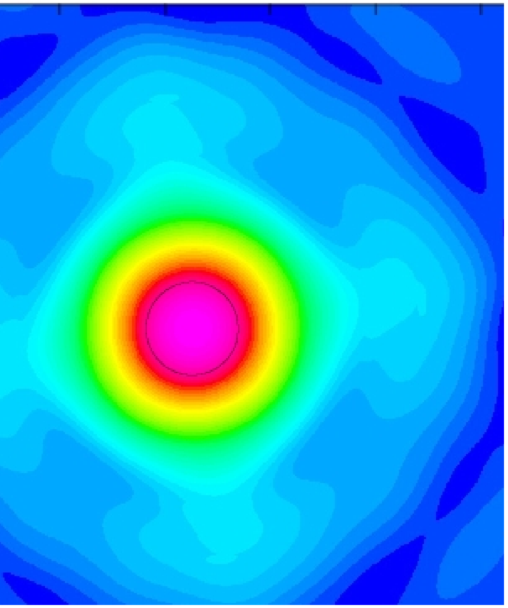

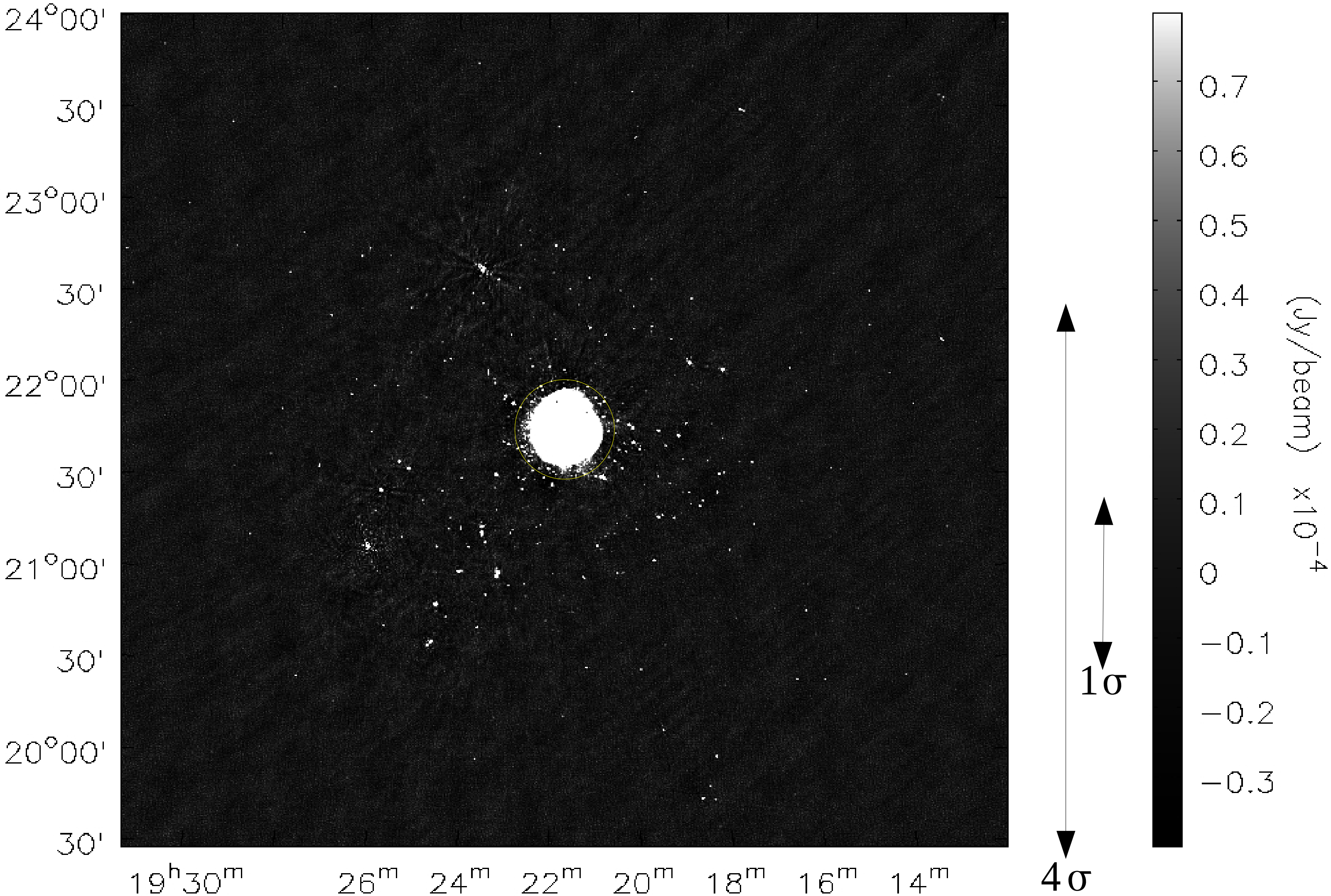

=> Wideband Imaging implies wide-field imaging

Wide Band

Wide Field

Full Beam

Wide Band + Full Beam

Example : Imaging the G55 supernova remnant

Summary

Wide Band + Full Beam Imaging – Algorithms

The measurement equation of an interferometer (per baseline) :

$$V_{ij}^{obs}(\nu,t) = M_{ij}(\nu,t) S_{ij}(\nu,t) \iiint M_{ij}^{s}(l,m,\nu,t) I(l,m,\nu,t) e^{2\pi i(ul+vm+w(n-1))} dl\, dm\, dn$$

Direction Independent Gains

- Eliminated during calibration

Primary Beams

- Power pattern varies with time, frequency and baseline

- PBcor (post-deconvolution)

- A-Projection

- WB-A-Projection

Sky-brightness varies with frequency (time)

- All sources have spectral structure (some vary with time)

– Cube Imaging

– Multi-Frequency Synthesis (MFS)

– Multi-Term-MFS

W-Term

-Non-coplanar baselines

-Sky curvature

– Faceting

- W-Projection

Iterative χ^2 minimization – Major and Minor Cycles

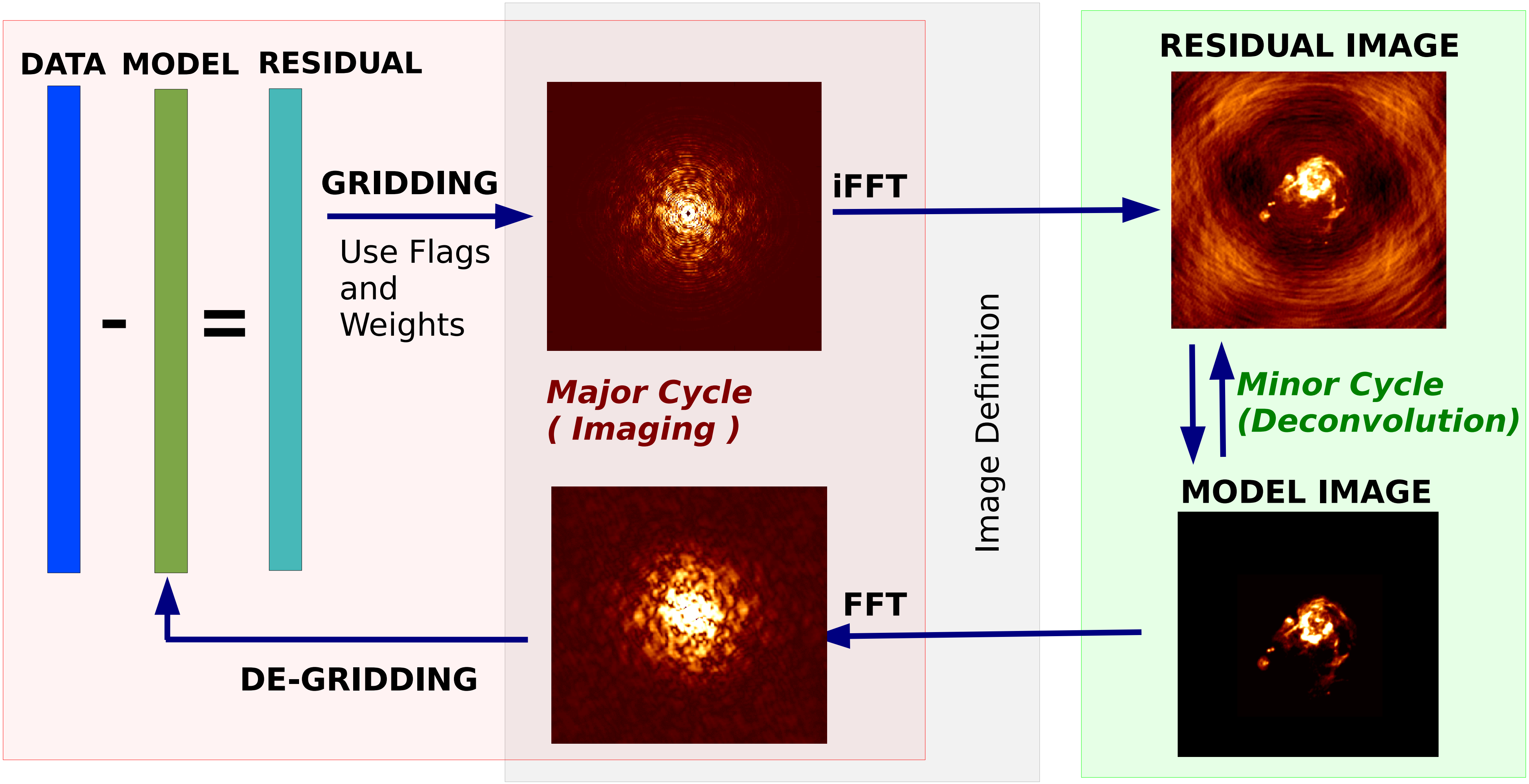

Standard gridding, W-Projection, (WB)-A-Projection, Joint Mosaics

Cube, MFS, MT-MFS, Faceting, Stokes, Multi-Field

Clean (Hogbom, Clark, MultiScale, MultiTerm, etc...)

Wide Band + Full Beam Imaging – Some guidelines

- MFS has better imaging fidelity, resolution and sensitivity than Cube

  -- For 2:1 bandwidth, the dynamic range limit with standard MFS (no spectral model) is few 100 to 1000 for a spectral index of -1.0

- MT-MFS gives HDR images when the spectral model is appropriate and there is sufficient SNR.

  -- For point sources, spectral index errors < 0.1 for SNR > 50 (2:1 bwr)
  for SNR > 10 (4:1 bwr)
  -- For extended emission, spectral index errors < 0.2 for SNR > 100

- W-Projection is more accurate and faster than Faceting

  -- For D-config,L-Band, uncorrected W errors are visible outside 1 deg

- PBcor assumes invariant beams, (WB)-A-Projection handles variability

  -- Uncorrected VLA beam squint and rotation causes DR < few x 10^4
  -- For 2:1 bwr, the PB's artificial spectral index at the HPBW is -1.4